T H E U N I V E R S I T Y O F M I C H I G A N

COLLEGE OF ENGINEERING
Department of Chemical and Metallurgical Engineering

Progress Report

NEW CONCEPTS ON UNDERGROUND STORAGE

M. Rasin Tek
J. O. Wilkes
D. A. Saville
L. Horton
Yu, Chin Uy
B. Bhalla

ORA Project 05625

under contract with:

THE AMERICAN GAS ASSOCIATION
NEW YORK, NEW YORK

administered through:

OFFICE OF RESEARCH ADMINISTRATION ANN ARBOR

May 1965

TABLE OF CONTENTS

LIST OF ILLUSTRATIONS

LIST OF ILLUSTRATIONS (Concluded)

CHAPTER 1

INTRODUCTION

The Project PO-50 "New Concepts on Underground Storage" was initialed at The University of Michigan during 1963 to "... formulate and explore new concepts" applied to underground storage of natural gas. The purpose of this report, the second annual progress report, is to present and discuss the progress up to date as well as the objectives for immediate and longer range future pertaining to the third and final year on the project. The research effort carried out during the second year of the project was devoted to three major areas designated in the original proposal. These were:

I. Detection and Remedy of Leaks from Conventional Storage Reservoirs

II. Soil Impermeation by Grouting

III. Underground Storage in Non-Porous Media

The original underground storage projects were located in depleted gas or oil reservoirs i.e. formations with well proved ability to retain hydrocarbons under pressure. While there were practically no underground storage reservoirs in the forties, depleted gas or oil field storage gained prominence during the fifties. Recently, in storing gas in such reservoirs a very significant breakthrough was made when the practice of "overpressuring" became a reality. The injection of gas into formations to pressure levels above the discovery resulted not only in large increases of the storage capacity of these fields but also paved the way to then unconventional but now conventional concept of "aquifer storage." A second breakthrough in gas

storage was made when the movement of water in contact with natural gas was quantitatively related to the performance of the gas storage bubble. By successfully applying high speed digital computing, significant new contributions were made to our understanding of the behavior of gas storage reservoirs subject to water drive. In this area along with new data, new solutions and contributions, a large number of new problems were uncovered. In the problem of overpressuring the physical processes leading to the development of the storage bubble during early stages of gas injection, drying of storage media by drainage of water between initial gas streamers, stability of gas fingering, elastic and mechanical properties of cap rocks related to breakage are among major fundamental problems yet to be solved. On the practical side the control of growth of gas bubble beyond areas of minimum structural closure, location, completion and treatment of observation wells, maintenance of storage reservoir boundaries within the limits of protective acreage by control of "cushion gas," optimum well density in heterogeneous storage reservoirs, interpretation of pressure survey data from non-homogeneous reservoirs are among problems of current, day-to-day interest. In the case of apparent leaks from storage reservoirs due to one reason or another the location, pressure testing and evaluation of possible collector zones is another problem of interest where field data must be analyzed with reservoir engineering calculations of special type.

In this report the problem of leakage will be approached from two viewpoints:

a. The mechanism of gas leakage across a cap rock studied on purely theoretical grounds by formulating a mathematical model describing the unsteady state two-phase flow through the porous matrix constituting the cap rock.

b. By specifically determining the effect of gas leakage on the performance of gas storage bubble as related to the movement of water in and out of the gas sand.

In the area of soil impermeation by grouting the experimental program carried out during the second year was directed to evaluate various grouts as to their effectiveness in sealing formations along controlled geometrics. It is well known that the success of aquifer storage depends critically on the presence of suitable subsurface geology.[1.1] Sufficient porosity, adequate permeability, satisfactory cap rock and complete structural closure are among the necessary requirements for aquifer storage. Even in areas where sedimentary rocks abound, the above factors do not always simultaneously co-exist. Sufficient porosity and permeability but lack of adequate structure or closure, adequate structure but leaky cap rock, semi open saddle structure or complete lack of anticline contour are examples of such imperfect conditions. The storage of gas in such strata requires artifical creation of boundaries impervious to the flow of natural gas. After reviewing during the first year on the project the existing methods of gas storage related to geographic, geologic and geophysical conditions to which they are best suited, the potential advantages of grouts applied through the porous media and from the surface of a cavity surrounded by porous media became apparent.[1.1] Study of various grouts available, determination of their desirable or undesirable physical properties, their effect on threshold pressures and their suitability to a particular type of formation have been the primary objectives of experi-

mental work carried out during the first two years and still in progress during the second.

In the area of unconventional underground storage, significant exploratory studies have been devoted to assess and evaluate the merits of several new concepts such as storage in dissolved salt caverns, in natural or mined caves, in cavities induced by nuclear explosions and finally underwater storage in the bottom of deep lakes and oceans.

In reporting the progress to date, the presentation of various topics mentioned above have been organized as independent chapters in a sequence approximately ranging from current and conventional interest to future, completely novel and unconventional aspects.

The second chapter consists of a comprehensive review of problems associated with leaks from conventional storage reservoirs subject to "overpressure." In this chapter the concept of overpressuring, its advantages as well as limitations are discussed in reasonable detail. The relation between capillary imbibition and drainage phenomena and leakage across cap rock, the concept of threshold pressure and problems related to mechanical fracturing of cap rocks are also included in Chapter 2.

The Chapters 3 and 4 relate to mechanism of gas leakage across cap rocks and to the performance of gas storage reserviors subject to leakage. The complete mathematical formulation of leak problem as two-phase two dimensional unsteady state flow across cap rocks is entertained in detail in Chapter 3. Equation which reconcile the material balances in gas inventory in the storage bubble with the movement of water in and out of the gas sand with

leakage occurring across the cap rocks are given in detail in Chapter 4.

The Chapter 5 presents the work currently underway on evaluation of grouts and reservoir engineering calculations related to grout injection.

The storage of natural gas in subsurface, non-porous storage cavities, unconventional methods and new concepts such as storage in cavities resulting from underground nuclear explosions and deep underwater storage near the bottom of oceans are featured in Chapter 6.

REFERENCES

1.1 New Concepts on Underground Storage, Progress Report 05625-1-P, University of Michigan, 1963.

CHAPTER 2

PROBLEMS ASSOCIATED WITH LEAKS FROM OVERPRESSURED STORAGE RESERVOIRS

The practice of operating storage reservoirs at pressures above the level corresponding to discovery of the particular field is called "overpressuring." During the last decade the storage capacity of and gas deliverability from a large number of depleted oil or gas producing reservoirs have been substantially increased through the practice of overpressuring. Early experiments with the practice of overpressure and simultaneous advances in our ability to understand and analyze the movement of water in contact with natural gas[2.1] led to the development of "aquifer storage" where the pore volume for storing natural gas was obtained through the expulsion of water from its native formation by injection of gas at pressures above the discovery pressure. Through proper applications of digital computation on high speed electronic computers, much has been added to our understanding of the performance of gas reservoirs subject to water drive.[2.2,2.3,2.4] These computational procedures which proved quite informative and practical revolved around the use of superposition principle to handle time varying boundary conditions, the material balances to reconcile the inventory gas in storage any time and unsteady state fluid flow equations describing the rate of movement of water in and out of the gas sand. These equations show that a storage reservoir maintained at "overpressure" over a long period of time will continue to grow. The rate of growth is found to be a function of physical, geometric, and geologic parameters of reservoir-aquifer system as well as the extent and duration of the "overpressure."

While such extended overpressure is usually practiced at early stages of development of storage reservoirs and is practiced with caution regarding the movement of gas water interface, it often causes concern in regard to spill of gas across areas of minimum structural closure. Judicious control of extent and duration of overpressure to delimit the areal expansion of the gas bubble and confine it to areas adequately covered by protective acreage is almost foremost in future planning of any storage operation. Field data gathered during the last decade on overpressured reservoirs also indicate on the other hand that just as effectively as the extended overpressure will continue to grow the gas storage bubble, operation at pressures below discovery or "underpressure" will shrink the gas bubble back to until safely within structural closure or protective acreage.

"Overpressure" viewed as a means to increase gas deliverability and storage capacity and "underpressure" as a means to control and contain the bubble within prescribed boundaries may be regarded as key factors entering into the overall logistics of a company's supply and transportation of natural gas. While one must recognize that increased deliverability on an existing system may also be obtained by means other than overpressuring such as development of new fields and peak-shaving storage capability, increased well density, increased well stimulation or more compression horsepower, the extent and nature of overpressure and underpressure operations must be analyzed on the basis of overall economic merits as well as current technical and practical engineering considerations.

2.1. Leakage or Spill from Overpressured Reservoirs

In deplected oil or gas reservoir storage or in "aquifer storage" the presence of a suitable cap rock is of paramount importance for the retention of natural gas within the structural boundaries of the reservoir. The cap rock that constitutes the overburden to a natural petroleum reservoir obviously does possess proved integrity to retain the gas at least up to discovery pressure. If overpressure conditions are sustained in a field, depending upon the extent of overpressure, possibility exists of gas leaking across the cap rock or moving in uncontrolled manner to formations beyond areas of minimum structural closure.

The leakage or spill of gas from a storage reservoir may be due to:

1. Exceeding the threshold pressure of the cap rock,
2. Mechanically fracturing the cap rock because of excessive overpressure
3. By having "overpressure" of excessive extent or duration to cause water to be pushed beyond the seal of structural closures
4. By fractures extending through and across the cap, induced during drilling or formation stimulation
5. By poor bonding of the cement between casing and hole
6. By existing permeable faults or incipient fractures in the native formation.

An excessive overpressure when sustained a long time, may cause the cap rock to leak or it may lift off the overburden causing nearly horizontal fracturing along bedding planes. Sometimes overpressure applied to deep wells may induce vertical fractures or oblique fractures as well. In aquifer storage the gas bubble is always at pressures

above the discovery pressure. The discovery pressure of a blanket sand containing water or petroleum reservoir containing hydrocarbon is usually related to the hydraulic gradient corresponding to the depth of the reservoir. Figure 2.1 shows the relationship between depth and discovery pressure for various petroleum reservoirs. It can be seen that the discovery pressure for most of the reservoirs lie between two limiting lines (A) and (B). The line (A) corresponds to the approximate upper limit corresponding to the weight of the overburden which is about 1.0 psi/ft. The line (B), the lower limit corresponds to the hydraulic gradient which is about 0.433 psi/ft for pure water.

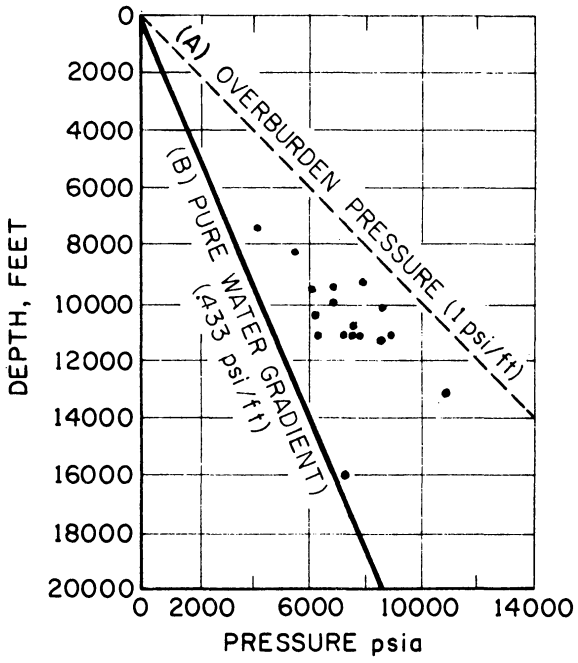

Fig. 2.1. Discovery and hydraulic pressure gradients for some fields.

The fact that most petroleum reservoirs are discovered at equilibrium values between the above 2 curves is considered in itself as a supporting evidence to theories of underwater sedimentation and compaction processes advanced by most geologists and petroleum engineers to explain the origin and

occurrence of petroleum deposits. The more or less minor variations frequently observed between the discovery and hydrostatic gradients are usually attributed to variations in the density of salt water and geothermal gradients existing on the crust of the earth. It must be recognized that it is not uncommon to observe discovery pressures outside the range delineated by curves (A) and (B). The abnormally high pressures are usually attributed to compaction of shales surrounding the strata bearing the hydrocarbons. The abnormally low pressures may be due to hydrology of underground water movement in as much as it may or may not communicate pressure wise without cropping strata.

It is generally accepted that a pressure gradient of 1 psi/ft is high enough to lift the overburden and will open a fracture along the bedding planes.

The difference of the limiting value of 1 psi/ft and the discovery gradient is basically the amount that brackets the extent to which "overpressure" may be available on a given field. For an aquifer 4000 feet deep, as an axample, this difference could be as high as 4000 (1 - 0.433) = 2270 psi.

For the example above somewhere between 1730 psia discovery and 4000 psia upper limit lies a safe and reasonable maximum pressure where overpressure can be safely and economically practiced.

In deciding the (psi/ft) at which the reservoir may be operated one must consider both the problems of leakage across the cap rock and breakage of the cap rock. It must also be pointed out that if storage is in semi-open

structures, the movement of water in the adjacent aquifer and the relation of water level to the spill point becomes equally important.

The problem of detection of leaks, and sealing of leaks in reservoirs through special techniques by soil impermeation are currently under study. The progress to date and current thinking on this area indicate that the leakage from cap rocks is related to water saturation in the cap as well as its imbibition and drainage characteristics related to capillary behavior.

The possibility of fracture of cap rock by mechanical failure due to pressure load on the gas bubble side may not be ignored for it may happen long before water is pushed out of the interstices of rock strata.

It appears that the relationship between "overpressure" and the leak phenomena, whether due to drying out of the cap or structural stress failure or excessive water movement, is the next logical area where some basic engineering research effort must be deployed.

The first break through in our understanding of gas storage reservoirs was accomplished when the reservoir pressure was quantitatively and correctly related to inventory gas quantities including the effect of water movement.

The second milestone was reached when it was discovered empirically that gas can be stored in aquifers and depleted reservoirs at pressures above the discovery.

The third break through, hopefully, would be containment of gas in large storage quantities through new concepts such as soil impermeation by artificial means.

The next logical effort toward adding more storage capacity to existing fields may be through the development of safe, reliable and rational methods permitting the quantitative evaluation of "overpressure" for each storage reservoir.

2.2. Concept of Threshold Pressure

Figure 2.2 shows a typical imbibition-drainage capillary pressure curve representing water distribution found in a reservoir standing over geologic times and consequently at capillary equilibrium. The threshold pressure noted on Fig. 2.2 is the pressure required for gas to start moving water out of the caprock previously fully saturated with water. In the drainage type of capillary pressure curve AB the two end points A and B are quite significant for our understanding of the performance of cap rocks. If the capillary pressure i.e., pressure difference between gas and water exceeds the threshold

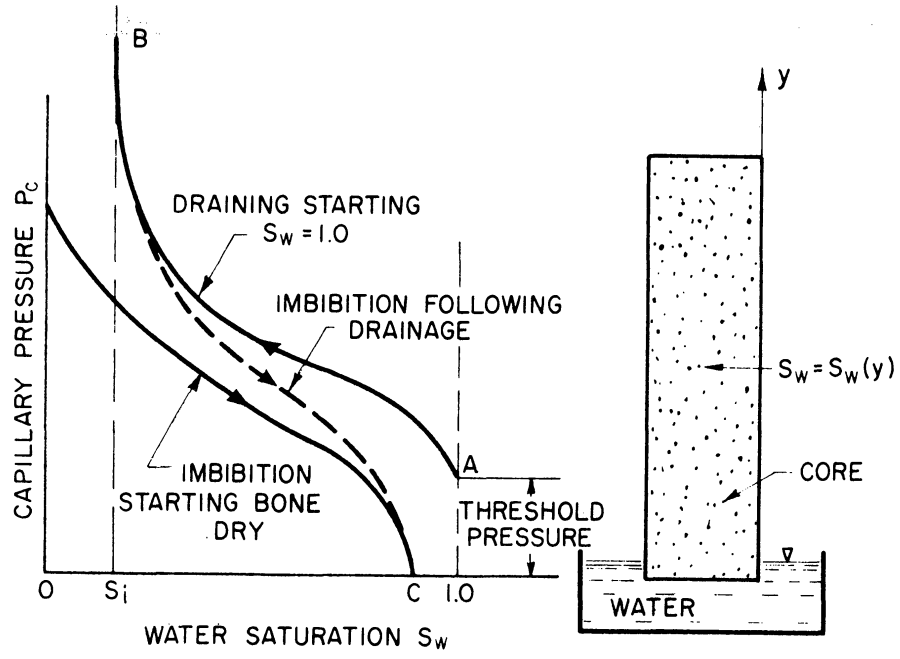

Fig. 2.2. Imbibition and drainage capillary pressure curves.

pressure the cap rock would lose its 100 percent water saturation and begin to leak along channels of high permeability. The other end point B where the saturation asymptotically approaches "connate water" saturation S_i is significant for the establishment of storage volume through the drying of sandstone in the aquifer. The value S_i is roughly correlated in the literature using the permeability as a parameter.[2.2,2.3] At present there exists no general correlation or method permitting the prediction of the threshold pressure from the first principles. An approximate correlation such as the one for connate water saturation has been developed by L. K. Thomas.[2.4] A recent attempt to predict the threshold pressure from the equation of general unsteady state two phase flow through porous media has not been conclusive.

Extensive laboratory data on samples of cap rock materials of high shale content and extremely low permeability is at present practically non-existent. Data on capillary pressures and the concept of relative permeability for tight cap rock materials are further subject to questionable accuracy and validity because of chemical effects associated with hydration of shales.

REFERENCES

2.1 Movement of Underground Water in Contact with Natural Gas, Katz, Tek, Coats, Katz, Jones, Miller AGA Monograph, Feb. 1963.

2.2 Schilthuis, R. J., "Connate Water in Oil and Gas Sands," Trans. AIME, 127, 199 (1938).

2.3 Katz, D. L., et al., Handbook of Natural Gas Engineering, McGraw Hill, (1959).

2.4 Michigan Gas Association Fellowship Report 1962-63.

CHAPTER 3

MECHANISM OF GAS LEAKAGE ACROSS A CAP ROCK

3.1. Introduction

The success of any project for storing gas in underground formations depends largely on locating a continuous natural barrier whereby the natural upwards motion of the gas may be restrained. Typically, such a barrier or "cap rock" will consist of a stratum of almost impervious shale; occasionally, sandstones and dolomites of very low permeability may also serve to prevent leakage. From the viewpoint of storing as much gas as possible in a given formation, it is desirable to overpressure the gas bubble so that its pressure considerably exceeds the formation discovery pressure. Clearly, the cap rock must possess both mechanical strength and an ability to withstand gas leakage. Only the latter property will be discussed in this chapter.

Upon discovery of a reservoir, the cap rock is usually fully saturated with water, to the extent that its minute porosity will allow. The presence of this water greatly enhances the ability of the cap rock to act as a seal against escaping gas. The pressure differential across the layer is fairly small, usually corresponding to that due to the ordinary hydrostatic gradient. A small increase in gas pressure on the undersurface of the cap rock will not cause an immediate leak. Rather, a certain threshold pressure, dictated by capillary forces within the cap rock, must be attained in the gas bubble before the gas starts to displace water. At a sufficiently high overpressure, the gas will work its way to displace water from permeable channels within the

cap rock and thus establish communication with the more porous and permeable formations above.

In practice, the gas bubble pressure will not always exceed the threshold pressure, but will vary with time (possibly in an approximately periodic manner) according to the particular injection production schedule. Uner these circumstances, the following questions may be asked:

(a) Will the gas displace water from the cap rock at all?

(b) If such a displacement occurs, will the gas penetrate the cap rock completely and thereby create a leak?

(c) Once a gas breakthrough has occurred, can water be reabsorbed into the cap rock by reducing the gas pressure?

(d) Is it possible for the gas/water interface to oscillate, so that it always remains within the cap rock?

(e) Is the interface sharply defined or diffuse in nature?

(f) Will the interface advance uniformly, or will there be a tendency for "fingering" to occur?

The discussion which follows will attempt to answer these questions. A more precise statement of the problem is presented in Section 3.3. First, however, we must consider the mathematical equations which describe immiscible two-phase flow in a porous medium.

3.2. Equations Governing Gas-Water Flow in a Porous Medium

The following notation will be used in this section. The introduction of specific units will be delayed until actual numerical calculations are made. For the present, it is understood that any consistent set of units may be employed.

Symbol	Definition
g	Gravitational acceleration.
h	Height.
k	Permeability.
k_g, k_w	Relative permeability for gas, water.
p_c	Capillary pressure, $p_c = p_g - p_w$.
p_g, p_w	Pressures in gas, water phases.
S	Water saturation, $S \equiv S_w$.
S_g, S_w	Gas and water saturations.
t	Time.
u_g, u_w	Superficial velocity vectors for gas, water, equal in magnitude to the volumetric flow rate per unit area normal to the flow.
ϵ	Porosity (fraction of total volume which is void).
μ_g, μ_w	Gas and water viscosities.
ρ_g, ρ_w	Gas and water densities.
ϕ_g, ϕ_w	Gas and water potentials, $\phi = p + \rho gh$.

The simplifying assumption is made that the gas and water behave as incompressible fluids. The following equations govern the two-phase flow.

Darcy's Law

For each phase, the superficial velocity vector is proportional to the potential gradient of that phase:

$$\vec{u}_w = - k \frac{k_w}{\mu_w} \nabla \phi_w \qquad (3.1)$$

$$\vec{u}_g = - k \frac{k_g}{\mu_g} \nabla \phi_g . \qquad (3.2)$$

Typically, the relative permeabilities k_g and k_w will depend on the water saturation in the manner shown in Fig. 3.1.

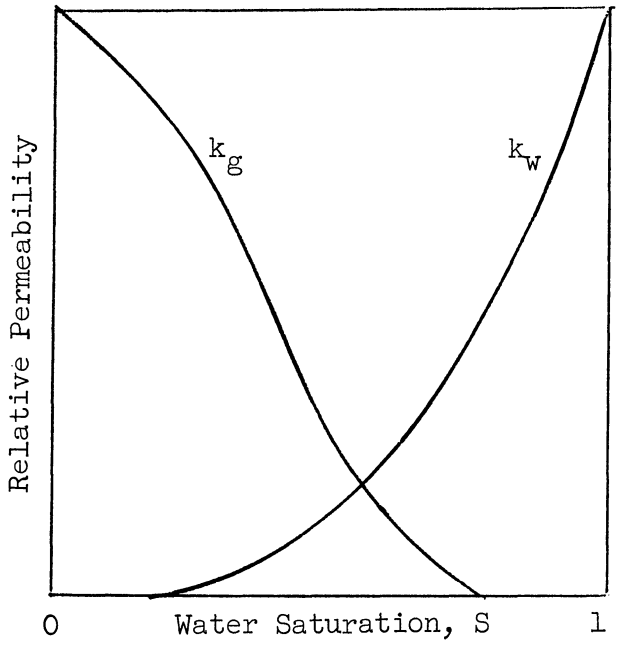

Fig. 3.1. Relative permeability.

Mass Balance

For each phase, the rate of accumulation per unit volume of medium equals the net rate of influx into that volume:

$$\epsilon \frac{\partial S_w}{\partial t} = - \nabla \vec{u}_w \quad \left(= \nabla k \frac{k_w}{\mu_w} \nabla \phi_w \right) \qquad (3.3)$$

$$\epsilon \frac{\partial S_g}{\partial t} = - \nabla \vec{u}_g \quad \left(= \nabla k \frac{k_g}{\mu_g} \nabla \phi_g \right). \qquad (3.4)$$

Relation between Saturations

The void spaces must be completely filled by water and/or gas, so that

$$S_w + S_g = 1. \tag{3.5}$$

Henceforth, we shall work mainly in terms of the water saturation S ($\equiv S_w$).

Capillary Pressure

The pressure in the gas phase exceeds that in the water by the capillary pressure:

$$p_c = p_g - p_w. \tag{3.6}$$

As indicated in Fig. 3.2, the capillary pressure depends on the water saturation and also on the direction of the displacement.

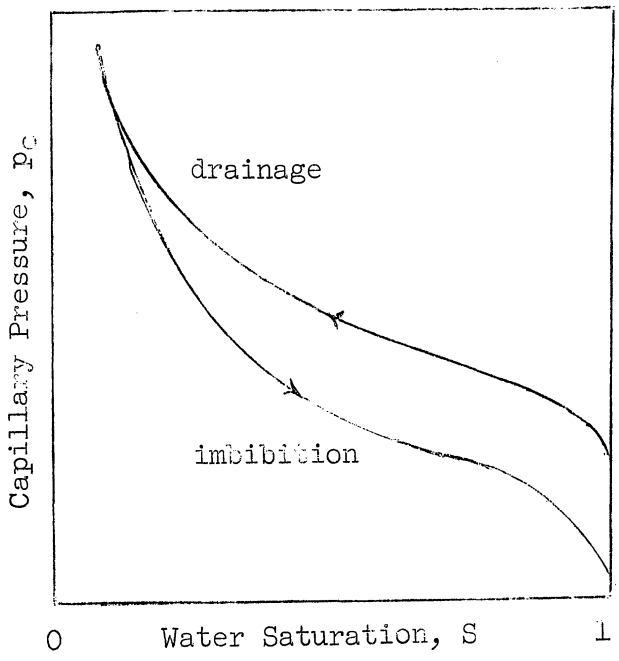

Fig. 3.2. Capillary pressure.

Definition of Potentials

$$\phi_w = p_w + \rho_w g h \tag{3.7}$$

$$\phi_g = p_g + \rho_g g h, \tag{3.8}$$

where h is the height above an arbitray datum. Note also the following relations:

$$\frac{\partial S}{\partial t} = \frac{dS}{dp_c}\frac{\partial p_c}{\partial t} \tag{3.9}$$

$$p_c = p_g - p_w = \phi_g - \phi_w + (\rho_w - \rho_g)gh \tag{3.10}$$

$$\frac{\partial p_c}{\partial t} = \frac{\partial(\phi_g - \phi_w)}{\partial t}. \tag{3.11}$$

Rearranged Equations

From Eqs. (3.3), (3.4), (3.5), (3.9), and (3.11), we obtain the following simultaneous non-linear partial differential equations in the water and gas potentials as the dependent variables:

$$\nabla k \frac{k_w}{\mu_w} \nabla\phi_w = \epsilon \frac{dS}{dp_c}\left(\frac{\partial\phi_g}{\partial t} - \frac{\partial\phi_w}{\partial t}\right), \tag{3.12}$$

$$\nabla k \frac{k_g}{\mu_g} \nabla\phi_g = -\epsilon \frac{dS}{dp_c}\left(\frac{\partial\phi_g}{\partial t} - \frac{\partial\phi_w}{\partial t}\right). \tag{3.13}$$

The saturation is actually a function of the two potentials since, if ϕ_w and ϕ_g are known, p_c is determined from (3.10) and S can then be found from the capillary pressure curve. Note that although Eqs. (3.12) and (3.13) will shortly be simplified, they hold generally for three-dimensional space.

3.3. Application of Equations to Leak Across Cap Rock

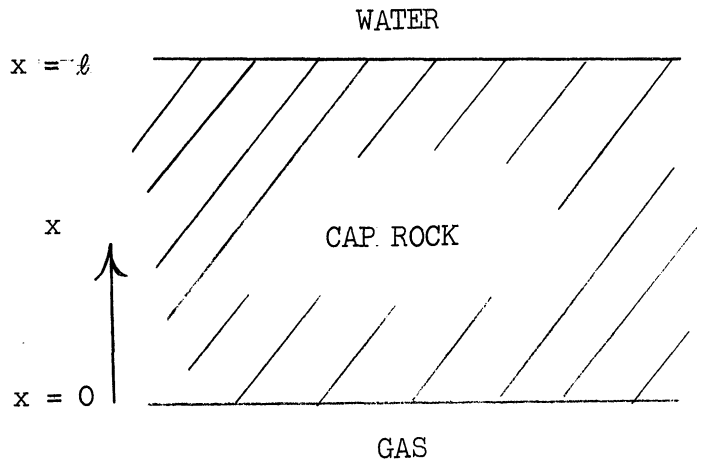

Fig. 3.3. Model for leak across cap rock.

Consider a horizontal cap rock of uniform thickness ℓ. Assume that the layer is bounded top and bottom by strata of much higher permeabilities which contain water and gas respectively. The potential of the water and gas above are maintained constant at values $\phi_{w\ell}$ and $\phi_{g\ell}$ respectively the potential of the gas below may, however, fluctuate with time, possibly in a periodic manner, according to some prescribed function $\phi_{g0}(t)$. At time t = 0, the cap rock is initially almost completely saturated with water.

Assume that no water flows down across the bottom face of the cap rock, but that gas may leak across the upper boundary. The motion will be treated as one-dimensional, in the vertical or x-direction. The problem is to determine the subsequent motion of gas and water in the cap rock.

For one space dimension, Eqs. (3.12) and (3.13) become

$$\frac{\partial}{\partial x}\left[k\,\frac{k_w}{\mu_w}\,\frac{\partial \phi_w}{\partial x}\right] = \epsilon\,\frac{dS}{dp_c}\left[\frac{\partial \phi_g}{\partial t} - \frac{\partial \phi_w}{\partial t}\right] \tag{3.14}$$

$$\frac{\partial}{\partial x}\left[k\,\frac{k_g}{\mu_g}\,\frac{\partial \phi_g}{\partial x}\right] = -\epsilon\,\frac{dS}{dpc}\left[\frac{\partial \phi_g}{\partial t} - \frac{\partial \phi_w}{\partial t}\right]. \qquad (3.15)$$

The associated initial and boundary conditions follow.

Initial Conditions ($t = 0,\ 0 \leq x \leq \ell$)

The water potential is constant throughout the cap rock and is equal to its value in the water just above the cap rock:

$$\phi_w = \phi_{w\ell}. \qquad (3.16)$$

The gas potential is also specified to be uniform throughout the cap rock at a level appropriate to the subsequent potential variations inside the gas bubble.

$$\phi_g = \phi_{g0}. \qquad (3.17)$$

The corresponding initial saturation distribution may be obtained by using the known capillary pressure saturation relation in conjunction with Eq. (3.10).

Boundary Conditions

The gas potential on the lower surface and both gas and water potentials on the upper surface are specified for all values of time:

$$\left.\begin{array}{lll} \text{At} & x = 0: & \phi_g = \phi_{g0}(t) \\ & x = \ell: & \phi_g = \phi_{g\ell} \\ & x = \ell: & \phi_w = \phi_{w\ell} \end{array}\right\} \qquad (3.18)$$

There is no flow of water across the lower boundary:

$$\text{At} \quad x = 0: \quad \partial\phi_w/\partial x = 0. \qquad (3.19)$$

An overall material balance must be satisfied. That is, the volumetric rate of injection of gas through the lower boundary equals the rate of displacement of water and gas through the top boundary, i.e.

$$q_{g0} + q_{g\ell} + q_{w\ell} = 0. \tag{3.20}$$

Here, the q's are considered positive for flow into the cap rock, with

$$\left.\begin{aligned} q_{g0} &= -\left[k\,\frac{k_g}{\mu_g}\,\frac{\partial \phi_g}{\partial x}\right]_{x=0} \\ q_{g\ell} &= \left[k\,\frac{k_g}{\mu_g}\,\frac{\partial \phi_g}{\partial x}\right]_{x=\ell} \\ q_{w\ell} &= \left[k\,\frac{k_w}{\mu_w}\,\frac{\partial \phi_w}{\partial x}\right]_{x=\ell} \end{aligned}\right\} \tag{3.21}$$

3.4. Equations in Terms of Dimensionless Variables

Note first that the relative permeabilities k_g and k_w, and the water saturation S are already dimensionless quantities. We next introduce dimensionless time, distance, potentials and capillary pressure defined by

$$\begin{aligned} T &= \frac{tk\phi_{w\ell}}{\ell^2 \epsilon \mu_w}, \qquad X = \frac{x}{\ell} \\ \Phi_g &= \frac{\phi_g}{\phi_{w\ell}}, \qquad \Phi_w = \frac{\phi_w}{\phi_{w\ell}}, \qquad P_c = \frac{p_c}{\phi_{w\ell}}. \end{aligned} \tag{3.22}$$

In terms of these new variables, the governing equations may be re-expressed in the following dimensionless forms.

Potential Equations

$$\frac{\partial}{\partial X} k_w \frac{\partial \Phi_w}{\partial X} = \frac{dS}{dP_c} \left(\frac{\partial \Phi_g}{\partial T} - \frac{\partial \Phi_w}{\partial T} \right) \tag{3.23}$$

$$\frac{\partial}{\partial X} k_g \frac{\partial \Phi_g}{\partial X} = - \frac{dS}{dp_c} \frac{\mu_g}{\mu_w} \left(\frac{\partial \Phi_g}{\partial T} - \frac{\partial \Phi_w}{\partial T} \right) \tag{3.24}$$

Initial Conditions At T=0, for $0 \leq X \leq 1$,

$$\Phi_w = 1$$

$$\Phi_g = \phi_{g\ell}/\phi_{w\ell}$$

The initial saturation distribution will be that corresponding to the starting dimensionless capillary pressure distribution computed from

$$P_c = \frac{\phi_{g\ell}}{\phi_{w\ell}} - 1 + \left\{ \frac{(\rho_w - \rho_g) g \ell}{\phi_{w\ell}} \right\} X. \tag{3.25}$$

Boundary Conditions For $T > 0$,

$$\left.\begin{array}{lll} \text{At} & X = 0: & \Phi_g = \Phi_{g0}(T) \\ & X = 0: & \partial \Phi_w / \partial_x = 0 \\ & X = 1: & \Phi_g = \phi_{g\ell}/\phi_{w\ell} \\ & X = 1: & \Phi_w = 1 \end{array}\right\} \tag{3.26}$$

Injection Rates

Dimensionless injection rates may be defined as

$$\left.\begin{aligned} Q_{g0} &= \frac{q_{g0}\mu_g \ell}{k k_g \phi_{w\ell}} = -\left(\frac{\partial \Phi_g}{\partial X} \right)_{x=0} \\ Q_{g1} &= \frac{q_{g\ell}\mu_g \ell}{k k_g \phi_{w\ell}} = \left(\frac{\partial \Phi_g}{\partial X} \right)_{x=1} \end{aligned}\right\} \tag{3.27}$$

$$Q_{w1} = \frac{q_w \mu_w \ell}{k k_w \phi_{w\ell}} = \left(\frac{\partial \Phi_w}{\partial X} \right)_{X=1} \tag{3.27}$$

Condition (3.20) then leads to

$$Q_{g0} + Q_{g1} + \frac{k_w}{k_g} \frac{\mu_g}{\mu_w} Q_{w1} = 0 \tag{3.28}$$

Equations (3.23) through (3.28), together with relations expressing relative permeabilities and capillary pressure as functions of saturation, constitute the problem statement. At the time of writing, these equations are being solved by a numerical finite difference technique. Details of the method of solution, and of the conclusions, will be presented in the final report.

The following is a summary of the additional notation which has been introduced in this section:

Symbol	Definition
ℓ	Thickness of cap rock.
P_c	Dimensionless capillary pressure.
q_g, q_w	Volumetric flow rates, per unit area, of gas and water into the cap rock, from below and above, respectively.
Q_g, Q_w	Dimensionless gas and water injection rates.
T	Dimensionless time.
x	Vertical distance above bottom of cap rock.
X	Dimensionless vertical distance.
$\phi_{g0}(t)$	Gas potential at lower surface.
$\phi_{w\ell}$	Water potential at upper surface (constant).
Φ_g, Φ_w	Dimensionless gas and water potentials.

CHAPTER 4

PERFORMANCE OF STORAGE RESERVOIRS SUBJECT TO LEAKAGE

Introduction

The purpose of this section is to investigate the effect of various types of cap rock leakage on the performance of storage reservoirs. Conversely, observations on reservoir performance may assist in pin-pointing a particular leak. Clearly, in such an investigation, allowance must be made for various types of gas seepage through the cap rock. For example, the leak may be very much localized, or it may be distributed over a wide area. The actual rate of leakage may be small or large, and may possibly not occur at all unless a certain threshold pressure is exceeded. Thus, several factors must be taken into account in formulating the leakage effect.

4.1. Model

We now specialize to the idealized situation illustrated in Fig. 4.1 which shows a horizontal gas bubble of uniform thickness and constant radius surmounted by a cap rock. The outer periphery of the gas bubble is taken to be impervious to gas flow, as is the rock formation underlying the reservoir. The single well-bore is subject to a variable pressure which is a known function of time. Since gas density increases with pressure, an increase in well pressure will cause additional gas to enter storage. The flow in the formation containing the bubble itself is taken to be in the radial direction only. The leakage rate through the cap rock is assumed to depend only on the particular

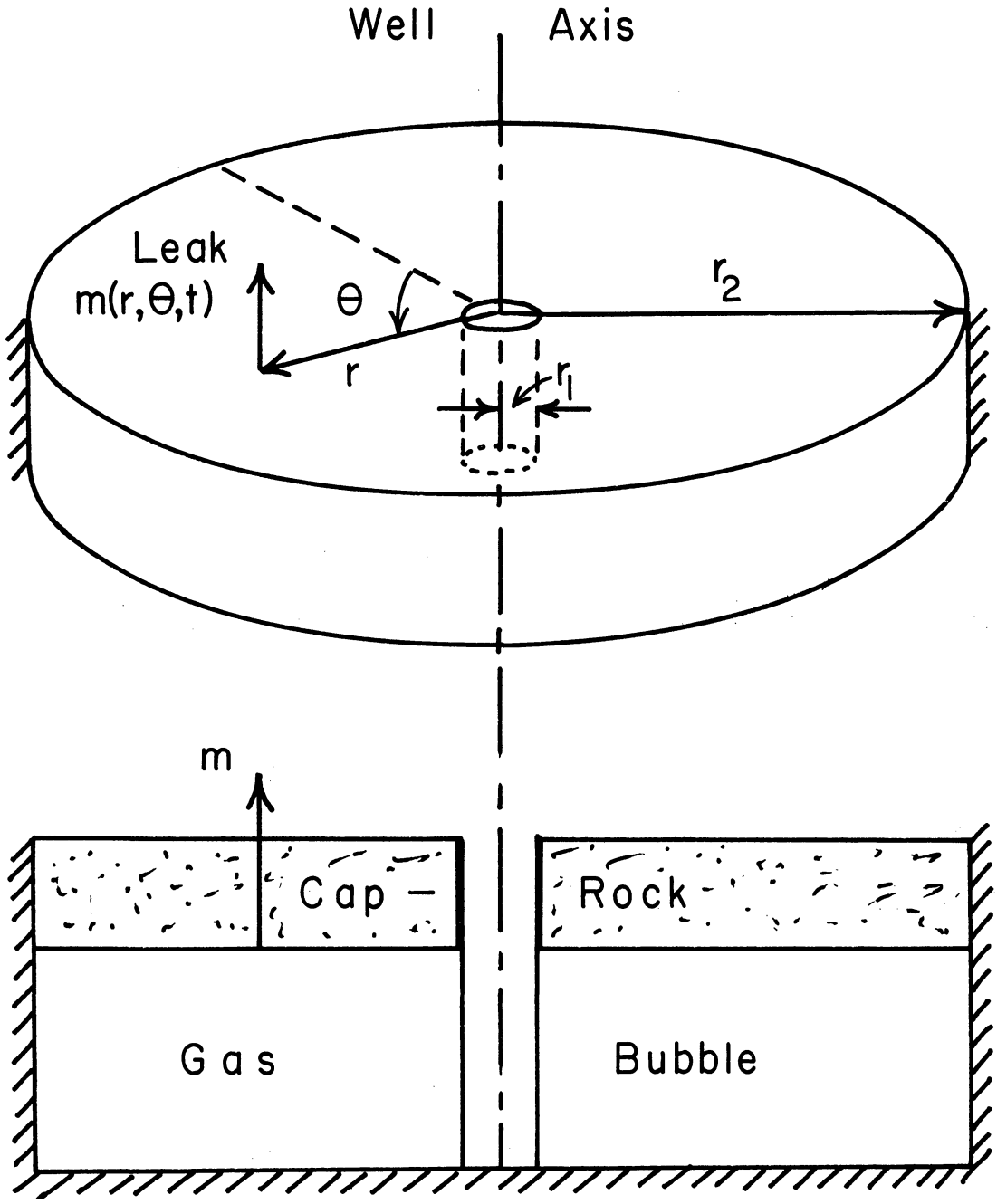

Fig. 4.1. Model for area-distributed gas leak.

radial position and on the prevailing local pressure in the gas bubble.

The problem is to determine the subsequent pressure variations in the gas bubble as functions of time and position.

Notation

k = Permeability of rock containing bubble.

ϵ = Porosity of rock containing bubble.

μ = Gas viscosity.

ρ = Gas density.

p = Pressure of gas in bubble.

t = Time.

v_r = Radial superficial velocity component.

v_θ = Angular superficial velocity component. (Later, we set $v_\theta = 0$).

r = Radial distance from center of well-bore.

r_1, r_2 = Radii of well and gas bubble.

m = Leakage mass flow rate per unit surface area of cap rock per unit depth of bubble.

For the present, assume that any consistent set of units is employed.

4.2. Governing Equations

Darey's law is obeyed in the radial and angular directions:

$$v_r = - \frac{k}{\mu} \frac{\partial p}{\partial r}, \tag{4.1}$$

$$v_\theta = - \frac{k}{\mu} \frac{1}{r} \frac{\partial p}{\partial \theta} . \tag{4.2}$$

The equation of continuity, taking into account raidal and angular flows,

accumulation due to density change and leakage through the cap rock, gives

$$\frac{1}{r}\frac{\partial}{\partial r}(\rho v_r r) + \frac{1}{r}\frac{\partial}{\partial \theta}(\rho v_\theta) + m = -\epsilon\frac{\partial \rho}{\partial t}. \tag{4.3}$$

The gas may be non-ideal, but is taken to obey the following simple equation of state:

$$\rho = cp, \tag{4.4}$$

in which c is a constant.

Eliminating v_r, v_θ and ρ between Eqs. (4.1), (4.2), (4.3) and (4.4), we obtain

$$p\frac{\partial^2 p}{\partial r^2} + \frac{p}{r}\frac{\partial p}{\partial r} + \left(\frac{\partial p}{\partial r}\right)^2 + \frac{p}{r^2}\frac{\partial^2 p}{\partial \theta^2} + \frac{1}{r^2}\left(\frac{\partial p}{\partial \theta}\right)^2 = \frac{m\mu}{kc} = \frac{\epsilon\mu}{k}\frac{\partial p}{\partial t}. \tag{4.5}$$

Dimensionless Form

It is convenient to introduce the following dimensionless variables.

Pressure: $P = \dfrac{p}{p_o}$

Time: $T = \dfrac{tkp_o}{\epsilon\mu r_1^2}$

Radius: $\eta = \dfrac{r}{r_1}$

Leakage rate: $M = \dfrac{m\mu r_1^2}{kcp_o^2}$

In the above, p_o refers to the initial uniform pressure throughout the reservoir. Equation (4.5) becomes

$$P\frac{\partial^2 P}{\partial \eta^2} + \frac{P}{\eta}\frac{\partial P}{\partial \eta} + \left(\frac{\partial P}{\partial \eta}\right)^2 + \frac{P}{\eta^2}\frac{\partial^2 P}{\partial \theta^2} + \frac{1}{\eta^2}\left(\frac{\partial P}{\partial \theta}\right)^2 - M = \frac{\partial P}{\partial T}. \tag{4.6}$$

Equation (4.6) is a non-linear second-order partial differential equation which governs transient variations of pressure with radial and angular positions inside the gas bubble.

Change of Variable

For the purpose of a later numerical finite difference solution, we also change the radial space variable to

$$R = \ell n\, \eta = \ell n(r/r_1).$$

Equation (4.6) is then transformed to give

$$P\frac{\partial^2 P}{\partial R^2} + \left(\frac{\partial P}{\partial R}\right)^2 + P\frac{\partial^2 P}{\partial \Theta^2} + \left(\frac{\partial P}{\partial \Theta}\right)^2 - Me^{2R} = e^{2R}\frac{\partial P}{\partial T}. \qquad (4.7)$$

The present investigation now considers pressure to be a function of radial location only. The simplified equation to be solved is thus

$$P\frac{\partial^2 P}{\partial R^2} + \left(\frac{\partial P}{\partial R}\right)^2 - Me^{2R} = e^{2R}\frac{\partial P}{\partial T}, \qquad (4.8)$$

in which

P = dimensionless pressure, p/p_o

R = dimensionless radius, $\ell n(r/r_1)$

T = dimensionless time, $tkp_o/\epsilon\mu r_1^2$

M = dimensionless leakage rate, $m\mu r_1^2/kcp_o^2$.

Boundary and Initial Conditions

The computer program written for the finite difference approximation to the solution of Eq. (4.8) can cope with any prescribed well pressure as a function of time and any radial distribution of leaks. For the purposes of comparing results in this investigation, it is expedient to consider the

following conditions.

Initially, the pressure is taken to be uniform and equal to p_o throughout the reservoir:

$$t = 0, \quad r_1 \leq r_2: \quad p = p_o.$$

For subsequent times, the well pressure p_1 is a prescribed function of time:

$$t > 0, \quad r = r_1: \quad p = p_1(t).$$

(One special case will be considered in particular, with well pressure maintained at a constant value p_w). The outer boundary of the bubble is impervious to gas flow:

$$t > 0, \quad r = r_2: \quad \partial p/\partial r = 0.$$

In dimensionless form, these initial and boundary conditions become

$$\left.\begin{aligned} &T=0, \quad 0 \leq R \leq \ell n(r_2/r_1): \quad P=1 \\ &T>0, \quad R=0; \quad P = p_1/p_o \\ &T>0, \quad R=\ell n(r_2/r_1): \quad \partial P/\partial R = 0 \end{aligned}\right\} \qquad (4.9)$$

4.3. Formulation of Leak

The type of leak still remains to be specified. A simple, yet fairly descriptive model is the following:

$$\left.\begin{aligned} m &= k^*(p-p_L) \qquad p > p_L \\ m &= 0 \qquad\qquad p \leq p_L \end{aligned}\right\} \qquad (4.10)$$

where m = leakage mass flow rate per unite cap rock surface area per unit depth of bubble,

p = local pressure in gas bubble,

p_L = threshold pressure below which no leak occurs,

k^* = coefficient depending on leakage rate.

Note that p_L and k^* may be functions of radius, so that the entire character of the leak may vary from one position to another.

In dimensionless form, we have

$$\left.\begin{aligned} M &= \left(\frac{k^*\mu r_1^2}{k\ c\ p_o}\right)\left(P - \frac{p_L}{p_o}\right), \qquad P > \frac{p_L}{p_o} \\ M &= 0, \qquad\qquad\qquad\qquad P \leq \frac{p_L}{p_o}\ . \end{aligned}\right\} \tag{4.11}$$

4.4. Results

In the preliminary results presented here, the following parameters are selected:

$\epsilon = 0.25$

$k = 50$ mullidarcies

$\mu = 0.05$ centipoise

$c = 0.003\ lb_m/(ft^3 psi)$

$r_1 = 0.25$ ft

$r_2 = 1000$ ft

$R_{max} = \ell n \frac{r_2}{r_1} = 8.294$

$p_o = 1000$ psi

$p_1 = 1200$ psi

$k^* = 0.1\ lb_m/(ft^3\ day\ psi)$

In the finite difference computation, the range R=0 to $R_{max} = 8.294$ is subdivided into ten equal increments by the introduction of eleven grid points. A localized leak is assumed to occur at the fifth grid point, corresponding to a leak spread over the fairly narrow range R/R_{max} from 0.45 to 0.55. Every-

where else, the cap rock is taken to be completely impervious to gas leakage.

As indicated above, the initial formation pressure is 1000 psi. The well pressure is then suddenly maintained at 1200 psi, corresponding to a dimensionless pressure P=1.2. Two types of leak are studied, with threshold pressures of p_L = 1000 and 1100 psi, shown in Figs. 4.2 and 4.3 respectively. These figures show how the pressure throughout the gas bubble varies with time. The corresponding curves for a completely impervious cap rock are also shown for purposes of comparison. These indicate a constantly increasing pressure which approaches P=1.2 uniformly for large values of time.

In the case of p_L = 1000 (Fig. 4.2), the effect of the leak is manifested very shortly. For radii beyond the leak, the pressure tends to become uniform as time increases. Note also that with the present coordinates it so happens that the pressure distribution is essentially linear on both sides of the leak, with a sharp change in slope at the leak itself. This suggests a method for detecting and pin-pointing a leak by making pressure recordings at just low observation wells. For, if the pressures are known at the points A, B, C and D of Fig. 4.2, then the intersection of AB and CD gives the location of the leak. The deviation between the slopes of AB and CD also depends on the magnitude of the leak. The final steady state of P=1.2 is never reached, since eventually all the gas being pumped into the well escapes through the cap rock. For the higher threshold pressure of p_L = 1100 (Fig. 4.3), the effect is again similar, but less pronounced.

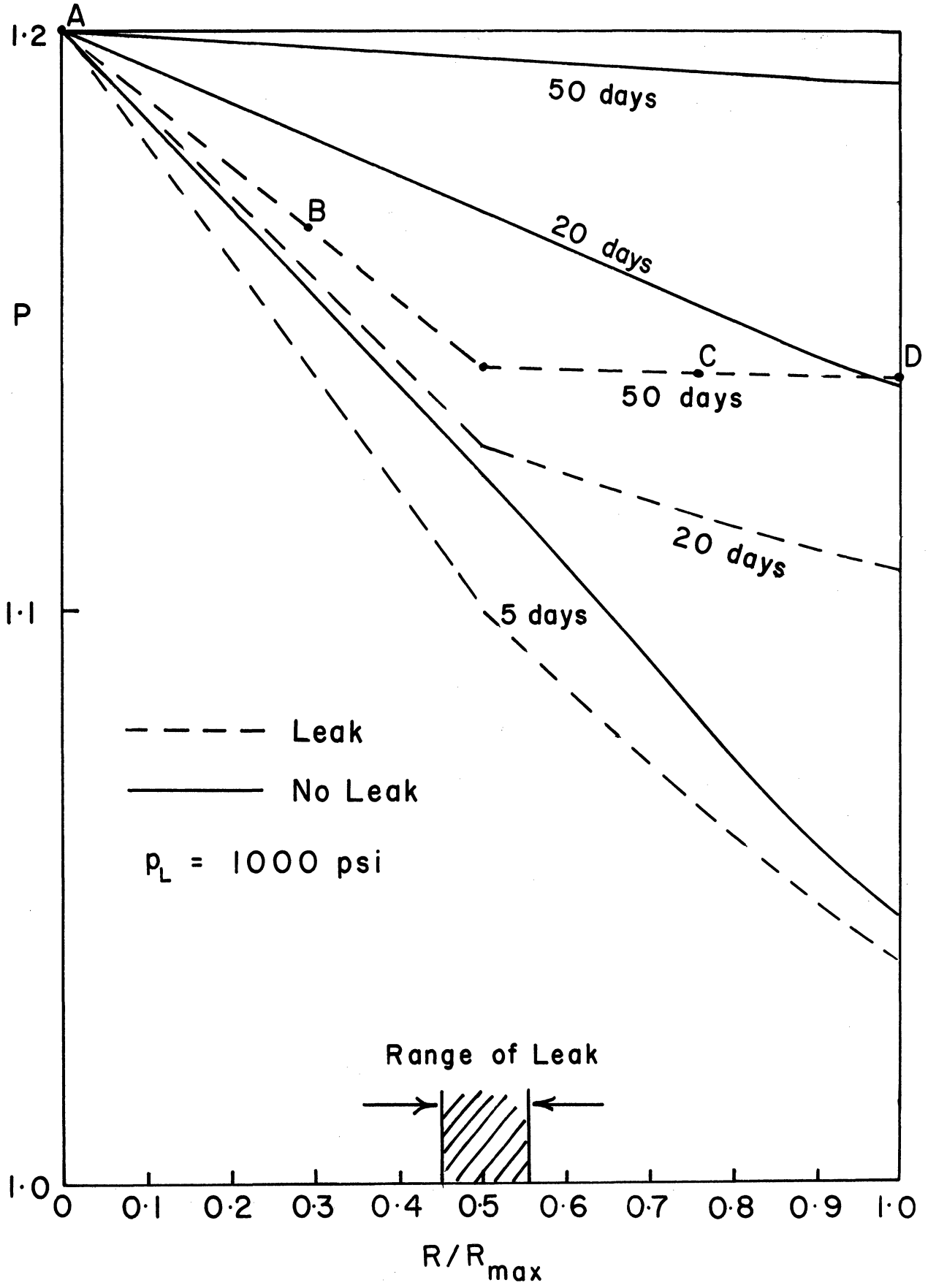

Fig. 4.2. Effect of leak on gas bubble pressure.

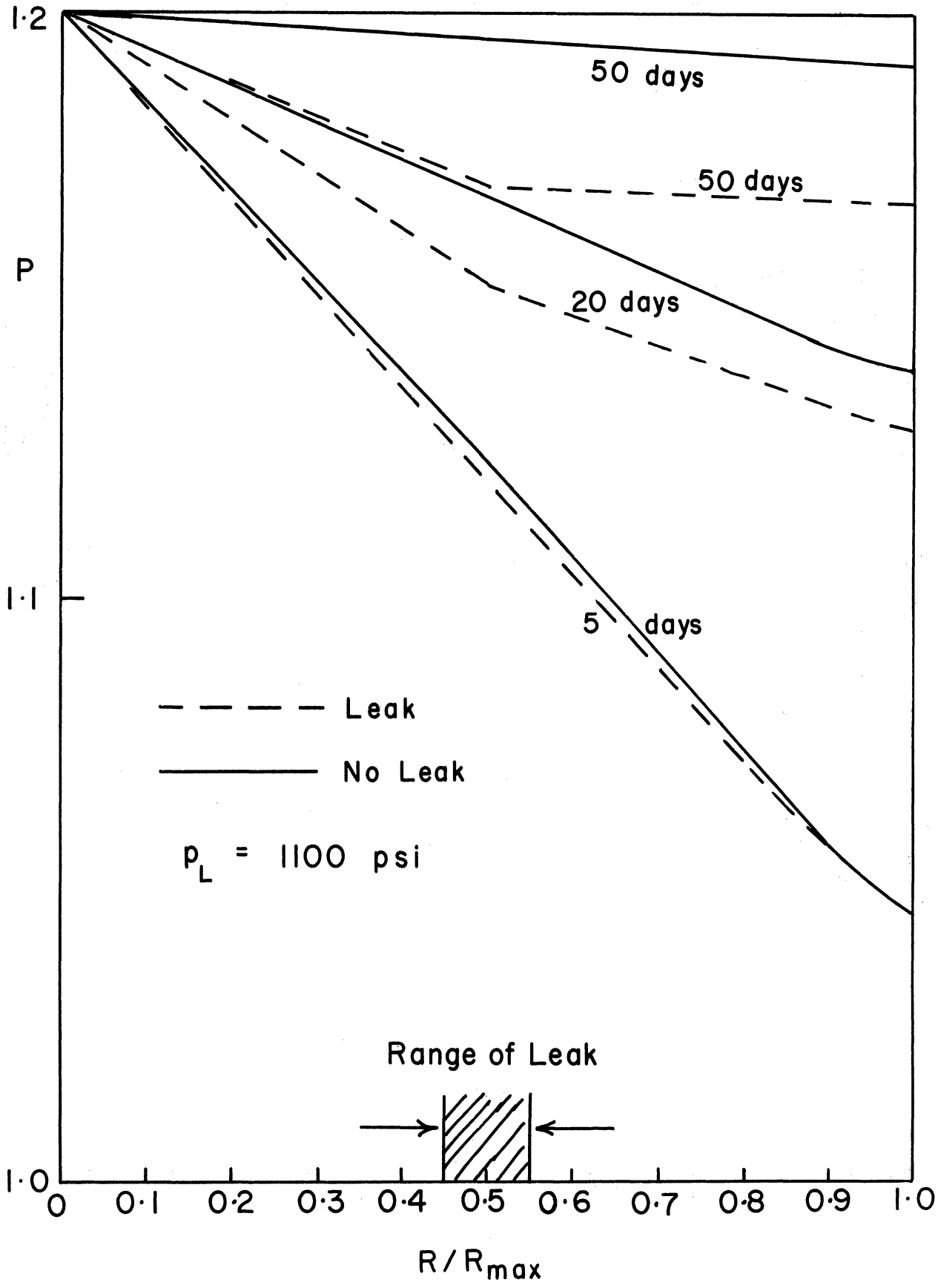

Fig. 4.3. Effect of leak on gas bubble pressure.

The one-dimensional model is obviously rather restrictive, and the method will next be extended to two dimensions. Also, the results will be put into a form more suitable for engineering calculations to be made.

CHAPTER 5

SOIL IMPERMEATION BY GROUTING

A review of all existing methods for underground storage of natural gas as related to geographic, geologic and geophysical conditions to which they are best suited suggested definite potential and interesting possibilities in the area of soil impermeation by grouting. The containment of a large storage bubble in underground strata having good porosity, good permeability but little or no structural closure or cap rock may indeed be possible if formations can be impermeated along controlled geometrics through injection of some chemical grouts. Figure 5.1 shows two areas where grouting materials may be applied in conventional underground storage. The cross section shows a semi-open structure where injection of the grout into the saddle area would definitely increase the storage capacity of the field beyond the "spill point" level.

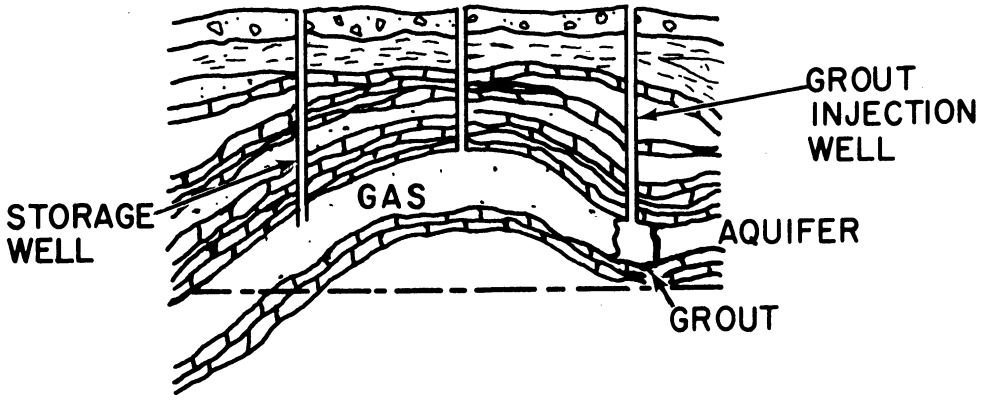

Fig. 5.1. Control of gas spill across saddle by grout injection.

When there is no cap rock or structure available the main problem in providing for the storage bubble centers upon impermeating the cap and lateral vertical boundaries by chemical grouts providing sufficient continuity and depth.

5.1. Evaluation of Grouts

The four major requirements for a grout to be used as a suitable material for soil impermeation are:

1. low viscosity while being pumped into the formation
2. controllable set time
3. quality to form a stable and impermeable gel
4. low cost

Various grouts commercially available or mixed and tested in the evaluation program are shown in Fig. 5.2. From the classification shown in Fig. 5.2 the suspension grouts are best suited for applications where surface impermeation is required. The suspension type materials will not penetrate through the pore structure of consolidated porous matrix. They will, however, provide good permeability barriers when applied to the surface of porous strata. They are expected to be used in problems of storage in mined or natural caverns, casing cement bond failure and other similar applications.

Of the true solution chemical grouts the ones which will polymerize in the pore matrix after having been injected offer the best possibilities in applications where impermeation is required in areal and depth continuity through the porous media. In the program directed toward evaluation of several grouting materials sandstone cores from typical formations, cap rock

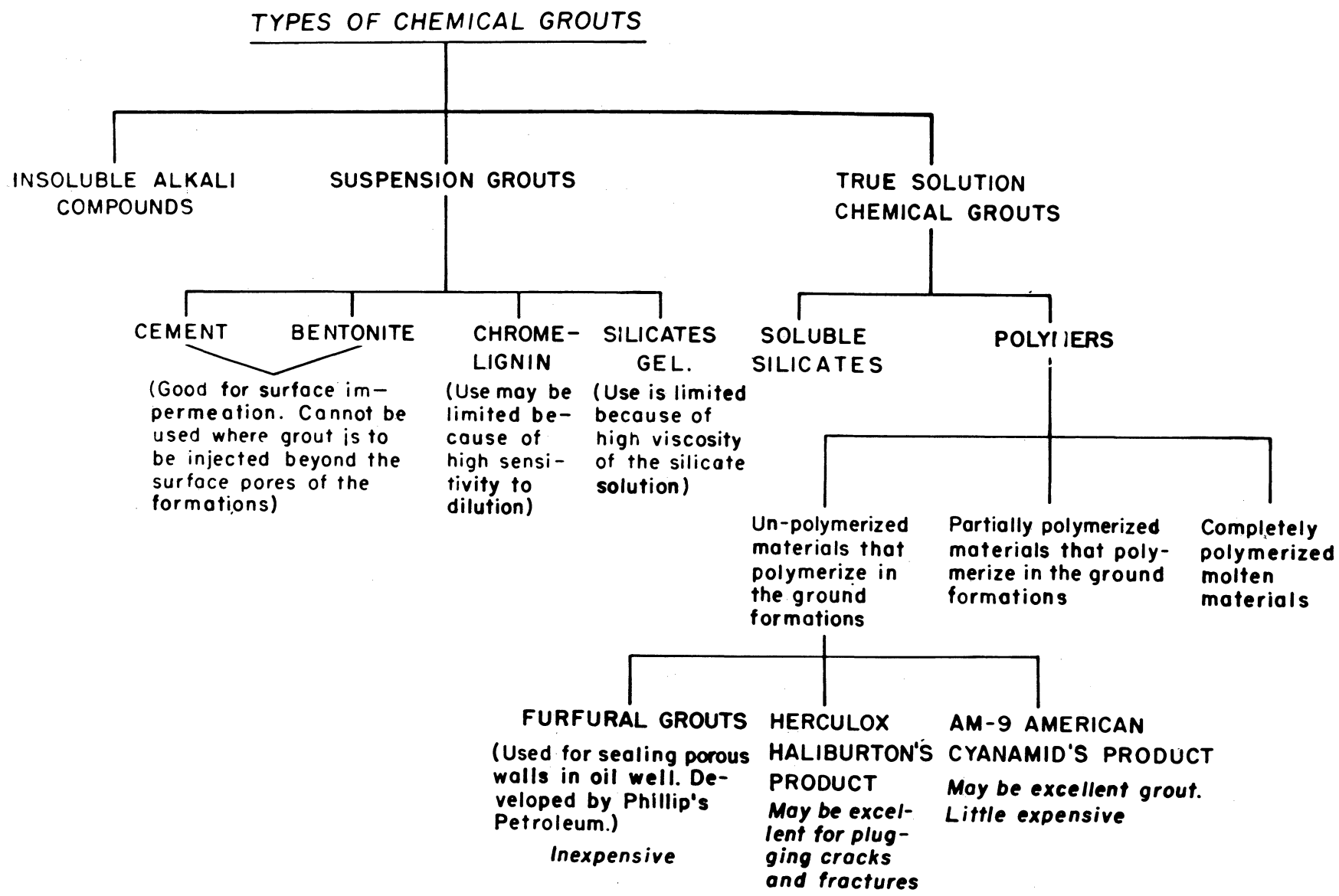

Fig. 5.2. Types of chemical grouts.

materials and specially prepared super-permeable sand-cement cores are used. The laboratory procedure on these include systematic measurements on porosity, permeability and threshold pressures before and after injection of grouts. The apparatus for these measurements in shown in Fig. 5.3. Figure 5.4 shows the layout diagram of various experiments used in evaluating the properties of cores and grouts. The time of polymerization of grout before the jel is set in the pore space is an important consideration and requires accurate and reliable data on the viscosity profile of the grouts. The equations used for determining the injectability of the grouts into the porous media involve as a first approximation single phase Newtonian flow with constant viscosity. The data on hand indicates that for some grouts, during the time of polymerization, the viscosity remains approximately constant for 3,4, up to 6 hours. A typical curve for the viscosity of a Siroc grout is shown in Fig. 5.5. It can be seen from this curve that for particular Siroc grout the viscosity remains quite constant at 6 centipoise level for about 4 hours before the grout starts to set. In reservoir calculations involving the injection of grouts radial and linear unsteady state single phase flow equations have been used to calculate the time dependent flow through porous media. For the types of grouting materials which show no period of constant viscosity, equations and solutions are being developed through the use of digital computers.

5.2. Reservoir Calculations of Grout Thickness and Injection Rate

The injection of solution into a porous medium to render the medium impervious to further fluid flow is called grouting. The grouting fluid

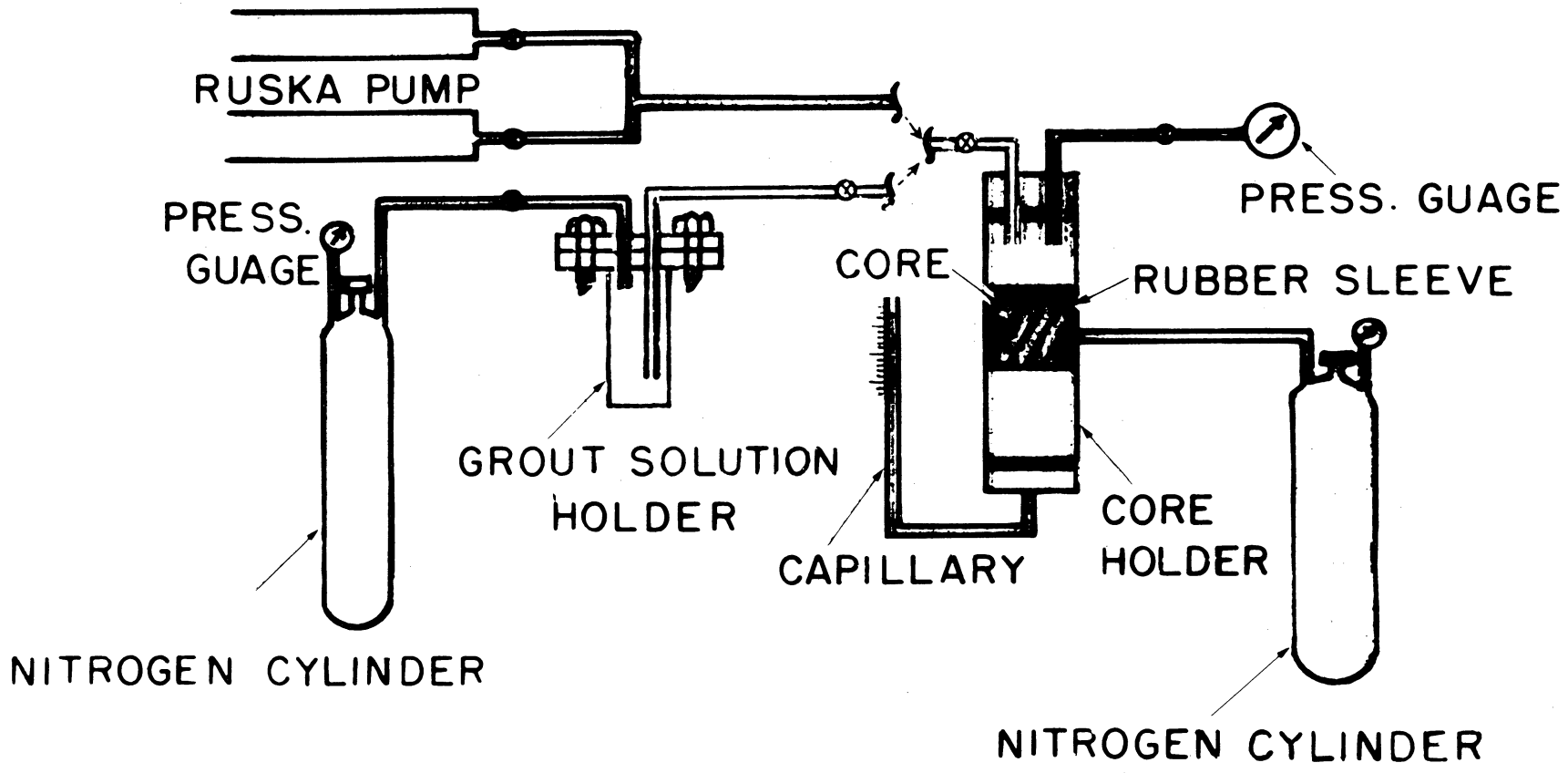

Fig. 5.3. Apparatus for evaluation of grout on actual core samples.

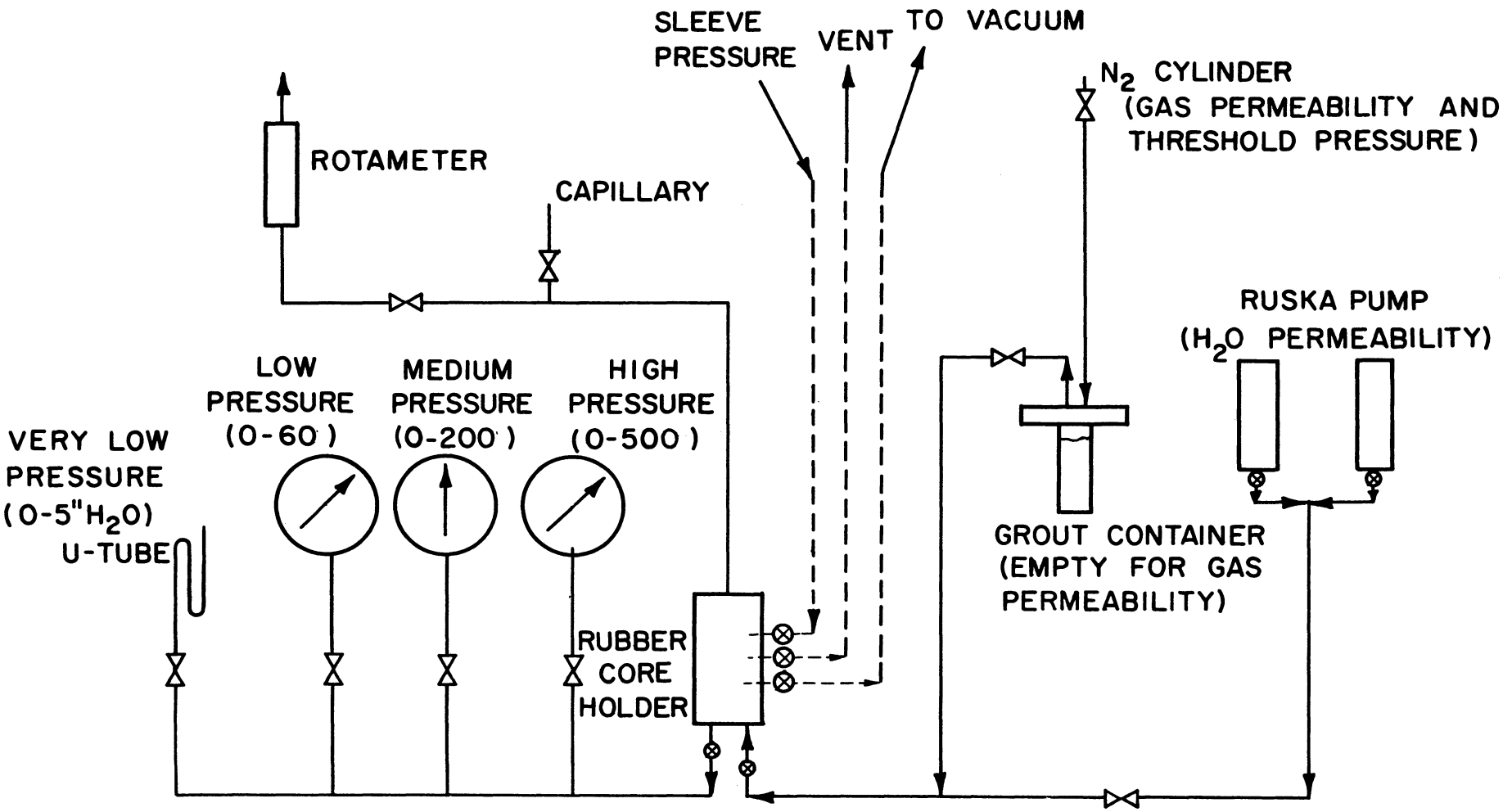

Fig. 5.4. Experimental layout of equipment used for evaluation of grouts.

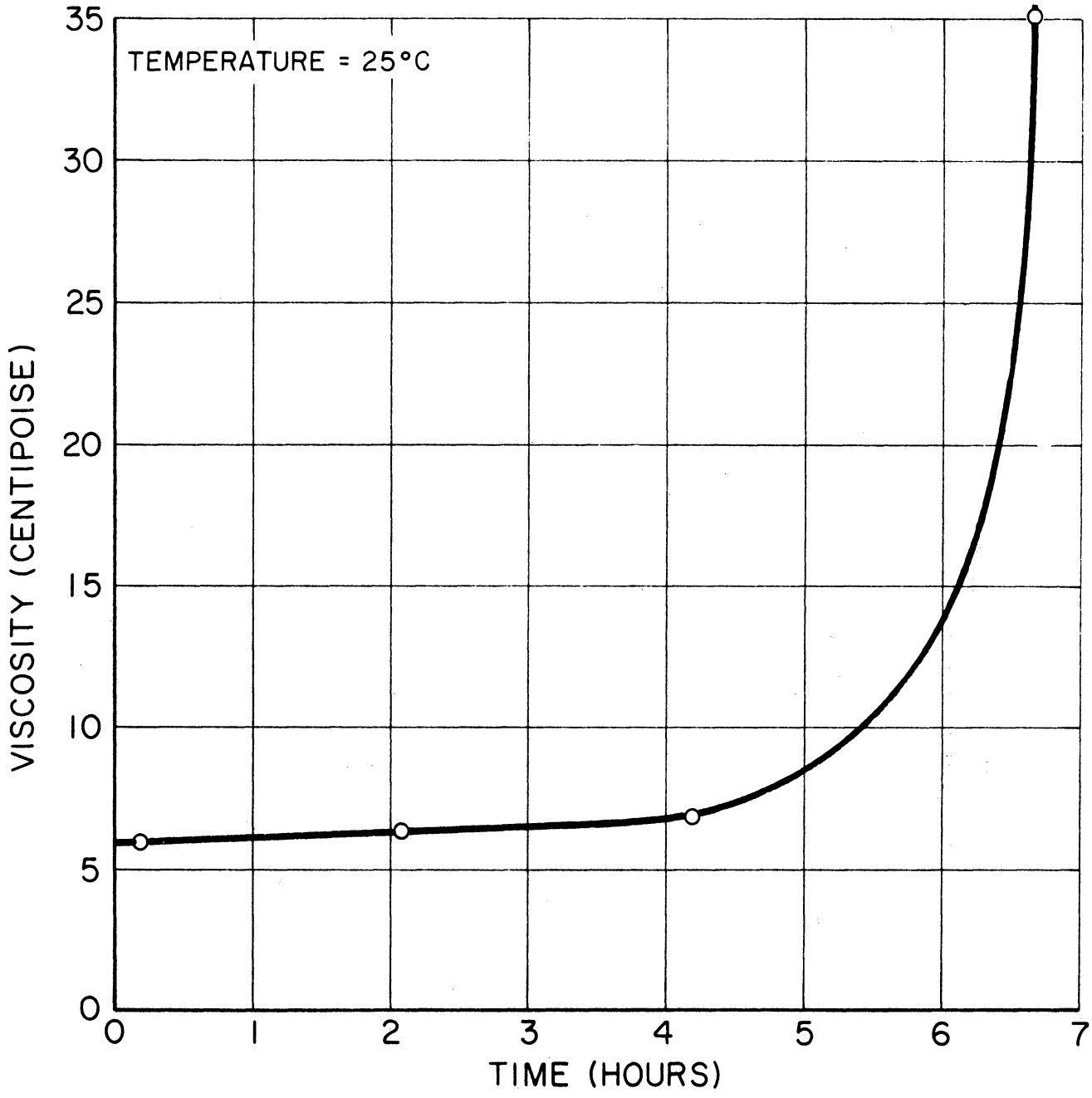

Fig. 5.5. Viscosity profile for Siroc grout.

undergoes a chemical change during and after the injection period. The resistence of the porous medium to further fluid flow may be measured in terms of a "threshold pressure." The threshold pressure being the maximum pressure difference which can be withstood without allowing fluid flow. The "strength" or threshold pressure of the grouted region depends on the thickness of this region (among other things). Hence the selection of a grouting material requires information about the rate of injection given the pressures, viscosities and other physical properties of the grout and the porous medium.

The objective of the study to be reported here is to predict the thickness of the impermeated region as it increases with the time elapsed since the start of the injection process given the following:

(a) viscosity-time relation for the grouting solution,

(b) viscosity of the fluid in place in the formation,

(c) permeability and porosity of the formation,

(d) compressibility of the porous material plus interstitial fluid,

(e) injection and formation pressures,

(f) shape of the grout front.

The problem is then one of calculating the displacement of one fluid (usually water) by another fluid (a grout solution). The major complication is due to the difference between the viscosities of the two fluids and the fact that the viscosity of the grouting fluid increases with time. A typical grouting fluid might have the viscosity-time behavior shown on Fig. 5.5.

Two types of fronts are being considered, planar and cylindrical. The planar front would apply to grouting from a plane fracture to produce vertical or horizontal boundaries while a cylindrical front would be encountered in grouting from a well to produce a vertical boundary.

Mathematical Models

The mathematical models used to describe the injection and displacement processes are based on the following primary assumptions

(a) superficial fluid velocity and pressure are related according to Darcy's Law,

(b) effects of capillary and gravitational forces can be neglected,

(c) injected and displaced fluids have the same density and compressibility,

(d) fluid-porous medium combination can be treated as slightly compressible,

(e) porous medium is homogeneous and isotropic,

(f) the interface between the injected and displaced fluids is a surface.

One short-coming of models based on these assumptions is that the effects of grout dilution due to molecular diffusion, bypassing of fluid in place and "fingering" are not accounted for. Hence the predicted grout thickness is probably greater than the "effective" thickness. However since grout solutions contain a large amount of water these effects are not expected to be large enough to invalidate the results.

The following notation will be employed in this chapter with the understanding that any consistent set of units may be employed.

A, B dimensionless constants

C compressibility of the fluid plus porous medium

k permeability

P local pressure

P_2 pressure at the injection surface

P_∞ pressure far from the surface

q volumetric injection rate per unit area

t time

$\dot{v}, \vec{v}$ superficial velocity, velocity vector

X coordinate normal to injection face

X_F position of front

ϵ porosity

K_1 $k/\mu_1 \epsilon c$

K_2 $k/\mu_2(t) \epsilon c$

λ parameter

μ_1 viscosity of fluid beyond the front

$\mu_2(t)$ viscosity of fluid between the front and the injection face (grout)

π 3.14159

ρ density

ρ_∞ density far from the injection face

ρ_2 density at injection face

$\nabla \cdot$ divergence operator, $i \frac{\partial}{\partial X} + j \frac{\partial}{\partial Y} + k \frac{\partial}{\partial Z}$

∇^2 Laplacian, $\frac{\partial^2}{\partial X^2} + \frac{\partial^2}{\partial Y^2} + \frac{\partial^2}{\partial Z^2}$

The continuity equation, Darcy's Law and the equation of state are

$$\epsilon \frac{\partial \rho}{\partial t} = \nabla \cdot (\rho \vec{v}) \tag{5.1}$$

$$\vec{v} = - \frac{k}{\mu} \nabla P \tag{5.2}$$

$$\rho = \rho_\infty e^{C(P-P_\infty)} \tag{5.3}$$

Then since

$$\nabla \rho = C \rho \nabla P \tag{5.4}$$

these equations may be combined to give a partial differential equation involving density, position and time as

$$\frac{\partial \rho}{\partial t} = \frac{k}{\mu \epsilon C} \nabla^2 \rho \tag{5.5}$$

In the "grouted" region the viscosity is denoted by $\mu_2(t)$ (a function of the time elapsed since the start of the injection process) and in the region beyond the interface by μ_1 (a constant). At the interface, $X_F(t)$, continuity of pressure and velocity result in

$$\rho(X_F^-, t) = \rho(X_F^+, t) \tag{5.6}$$

$$v(X_F^-, t) = v(X_F^+, t) \tag{5.7}$$

Equation (5.5) applied to the two regions of interest (between the injection point and the interface and beyond the interface) and the continuity conditions, (Eqs. (5.5) and (5.7)) are assumed to describe the flow processes. These equations, along with certain initial and boundary conditions, will predict the front movement (grout thickness) given the data specified in the previous section.

Equations Describing Grout Injection in One Dimension

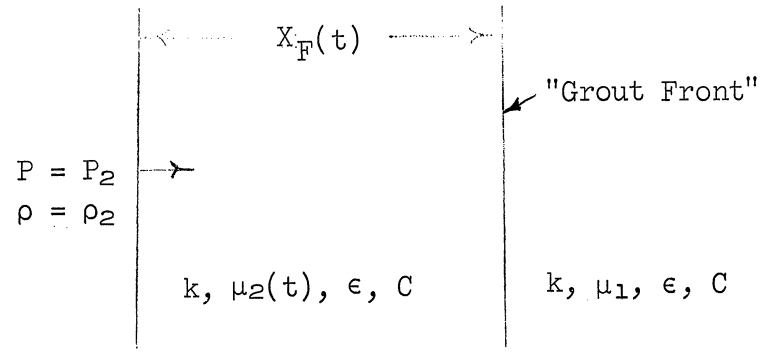

Fig. 5.6. Coordinate system for "linear grouting."

The geometry is indicated on Fig. 5.6. The grout front is assumed to move as a plane, its position noted as $X_F(t)$. Initially the semi-infinite region is at some uniform pressure (P_∞) and contains a fluid with viscosity μ_1. The pressure at the plane of the origin is raised to a level $P_2 (P_2 > P_\infty)$ and kept there. The grouting solution, viscosity $\mu_2(t)$, begins to invade the porous medium. The viscosity of the grouting solution depends only on the elapsed time measured from the start of the injection process. The local density may be found from the solution of the following problem in partial differential equations.

$$\frac{\partial \rho}{\partial t} = K_2(t) \frac{\partial^2 \rho}{\partial X^2} \qquad 0 < X < X_F(t) \tag{5.8}$$

$$\frac{\partial \rho}{\partial t} = K_1 \frac{\partial^2 \rho}{\partial X^2} \qquad X_F < X \tag{5.9}$$

where

$$K_2(t) = k/\mu_2(t)\epsilon C$$

$$K_1 = k/\mu_1 \epsilon C \tag{5.10}$$

with

$$t = 0 \qquad \rho = \rho_\infty, \quad P = P_\infty, \quad X_F = 0 \tag{5.11}$$

$$t > 0 \qquad \rho = \rho_2, \quad P = P_2 \text{ at } X = 0 \tag{5.12}$$

$$\rho(X_F^-, t) = \rho(X_F^+, t) \tag{5.13}$$

$$\left(\frac{\partial P}{\partial X}\right)_{X_F^-} = \frac{\mu_2(t)}{\mu_1}\left(\frac{\partial P}{\partial X}\right)_{X_F^+} \tag{5.14}$$

$$\rho \to \rho_\infty \text{ as } X \to \infty \tag{5.15}$$

This problem is difficult to solve for $\mu_2(t)$ an arbitrary function of time and numerical methods will be employed, however, for $\mu_2(t)$ constant an analytical solution is possible. Furthermore the solution has an interesting physical interpretation which should aid in the investigation of the problem in cylindrical coordinates and explain some of the numerical results.

5.3. Solution for a Constant Viscosity Grout Solution—Plane Front

The grout solution is assumed to have a constant viscosity μ_2 ($\mu_2 > \mu_1$) for a period of time after which the viscosity increases rapidly.

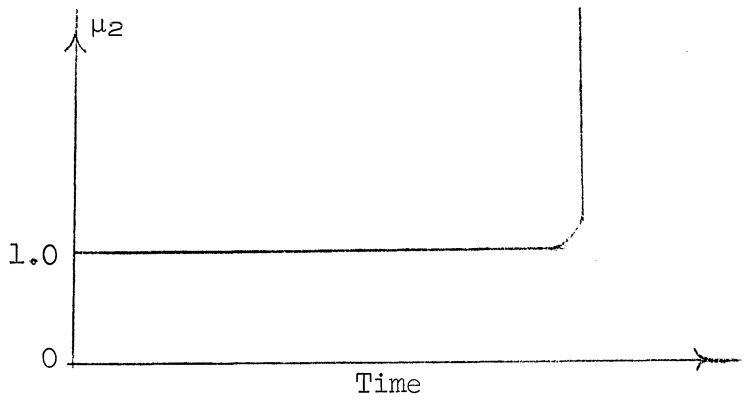

Fig. 5.7. Viscosity-time curve.

The partial differential equations and all boundary and initial conditions except at the front are satisfied by

$$\frac{\rho-\rho_\infty}{\rho_2-\rho_\infty} = 1 + A\ \mathrm{erf}\left(\frac{X}{2\sqrt{K_2 t}}\right) \quad 0 < X < X_F \tag{5.16}$$

$$\frac{\rho-\rho_\infty}{\rho_2-\rho_\infty} = B\ \mathrm{erfc}\left(\frac{X}{2\sqrt{K_1 t}}\right) \quad X_F < X \tag{5.17}$$

where "erf" and "erfc" denote the error function and complimentary error function respectively. The constants A and B are found from the conditions at the front namely,

$$1 + A\ \mathrm{erf}\left(\frac{X_F}{2\sqrt{K_2 t}}\right) = B\ \mathrm{erfc}\left(\frac{X_F}{2\sqrt{K_1 t}}\right) \tag{5.19}$$

$$\frac{A}{(\mu_2)^{1/2}} = -\frac{B}{(\mu_1)^{1/2}} \exp\left[-\frac{X_F^2}{4t}\left(\frac{1}{K_1} - \frac{1}{K_2}\right)\right] \tag{5.20}$$

If both of these conditions are to hold for all values of time then the equation for the movement of the front must be

$$X_F = 2\lambda(K_1 t)^{1/2} \tag{5.21}$$

where λ is a constant to be determined. It may be noted in passing that this problem is quite similar in structure to the "freezing front" problem discussed by Carslaw and Jaeger.[5.1]

From (5.19) and (5.20)

$$A(\lambda) = -\left\{\left(\frac{\mu_1}{\mu_2}\right)^{1/2} \exp\left[\lambda^2\left(1 - \frac{\mu_2}{\mu_1}\right)\right]\mathrm{erfc}(\lambda) + \mathrm{erf}\left(\lambda\left(\frac{\mu_2}{\mu_1}\right)^{1/2}\right)\right\}^{-1} \tag{5.22}$$

$$B(\lambda) = \left\{\operatorname{erfc}(\lambda) + \left(\frac{\mu_2}{\mu_1}\right)^{1/2} \exp\left[-\lambda^2\left(1 - \frac{\mu_2}{\mu_1}\right)\right]\operatorname{erf}\left(\lambda\left(\frac{\mu_2}{\mu_1}\right)^{1/2}\right)\right\}^{-1} \tag{5.23}$$

Since the movement of the front is given by Darcy's Law

$$v = -\frac{k}{\mu_1}\left(\frac{\partial P}{\partial X}\right)_{X_F^+} = -\frac{k}{\mu_1 C}\left(\frac{1}{\rho}\frac{\partial \rho}{\partial X}\right)_{X_F^+} \tag{5.24}$$

We have

$$\lambda = \frac{B(\lambda)}{\pi^{1/2}}\,\epsilon\, e^{-\lambda^2}\,\frac{(\rho_2-\rho_\infty)}{\rho(X_F,t)} \tag{5.25}$$

where $\rho(X_F,t)$ is found from either (5.16) or (5.17). Since

$$\frac{\rho_2-\rho_\infty}{\rho(X_F,t)} = \frac{e^{C(P_2-P_\infty)}-1}{1+(e^{C(P-P_\infty)}-1)\,B(\lambda)\operatorname{erfc}(\lambda)} \tag{5.26}$$

it can be seen that λ depends on three dimensionless parameters, ϵ, $C(P_2-P_\infty)$ and μ_2/μ_1. For small values of $C(P_2-P_\infty)$ and $\mu_2/\mu_1 \sim 1$ the result is

$$\lambda \doteq \frac{\epsilon C(P_2-P_\infty)}{(\pi)^{1/2}} \tag{5.27}$$

Hence the position of the front is approximately

$$X_F \doteq 2(P_2-P_\infty)\left(\frac{k\epsilon C}{\pi\mu_1}\right)^{1/2} t^{1/2} \tag{5.28}$$

This is, of course, the same result as would have been obtained if the injected fluid were considered to have the same viscosity as the fluid in place. Since $C(P_2-P_\infty)$ is usually small due to the compressibility of the formation it is of interest to find the error between this result and the exact result for $\mu_2/\mu_1 > 1$. The implication being that the rate of front movement may be controlled by $C(P_2-P_\infty)$ rather than by the viscosity ratio.

The roots (λ) of Eq. (5.25) are shown in the following table for several values of μ_2/μ_1.

TABLE 5.1

ROOTS OF EQUATION (5.25)

$C(P_2-P_\infty) = 7.938 \times 10^{-3}, \quad \epsilon = .15, \quad \epsilon C(P_1-P_\infty)/\pi^{1/2} = 6.72 \times 10^{-4}$

μ_2/μ_1	λ
1	6.691×10^{-4}
2	6.686×10^{-4}
3	6.681×10^{-4}
4	6.676×10^{-4}
5	6.671×10^{-4}
6	6.666×10^{-4}
7	6.661×10^{-4}
8	6.656×10^{-4}
9	6.652×10^{-4}

The error in the approximate result is seen to be small.

The previous result may be interpreted by considering the injection rate in the following manner. The rate, q, in units of volume injected per unit area per unit time is given by

$$q\rho_2 = \epsilon \underbrace{\int_0^{X_F} \frac{\partial \rho}{\partial t}\, dX}_{①} + \epsilon \underbrace{\int_{X_F}^{\infty} \frac{\partial \rho}{\partial t}\, dX}_{②} \tag{5.29}$$

Terms 1 and 2 represent the rate of change of mass in the regions on either side of the front. From the exact solution the result is

$$q\rho_2 = \epsilon(\rho_2-\rho_\infty)\left(\frac{K_1}{\pi t}\right)^{1/2}\left[A(\lambda)\left(\frac{\mu_1}{\mu_2}\right)^{1/2}\left(e^{-\lambda^2\,\mu_2/\mu_1}-1\right)+B(\lambda)\,e^{-\lambda^2}\right] \tag{5.30}$$

For $C(P_2-P_\infty)$ small

$$\frac{\rho_2-\rho_\infty}{\rho_2} \sim C(P_2-P_\infty) \qquad (5.31)$$

Hence the rate of injection from (5.30) is

$$q \sim \epsilon C(P_2-P_\infty)\left(\frac{K_1}{\pi t}\right)^{1/2}\left\{A(\lambda)\left(\frac{\mu_1}{\mu_2}\right)^{1/2}\left(e^{-\lambda^2\,\mu_2/\mu_1}-1\right)+B(\lambda)e^{-\lambda^2}\right\} \qquad (5.32)$$

For λ small this reduces to the same rate given by Eq. (5.28). The conclusion is that the rate of injection in this instance (λ small) is controlled entirely by the rate of "compression" in the region beyond the front and viscosity plays a minor role in the region between the injection face and the front.

This interpretation is of importance in that it may provide an approximation method for situations where no analytical solutions are available (cylindrical coordinates a viscosity varying with time).

5.4 Conclusions and Discussion of Work in Progress

A possible simplification of the description of the grout injection process has been found and verified for the case of a constant viscosity grout solution. If this simplified description can be justified for the case of a grout having a time dependent viscosity then approximate solutions for the rate of front movement can be obtained from known, tabulated solutions.[5.2]

The present effort in this area is directed towards numerical solution of governing equations for injection of a fluid with a time dependent viscosity. These results will be reported and compared with those from the approximation technique in the final report.

In order to provide impermeable boundaries horizontally across the top and vertically along the lateral periphery the economics of grouting would

indeed be enhanced if the injection of grout is combined by formation of horizontal and vertical fractures along the planes of controlled geometry. Recent advances in the technology of fracturing indicate that a great degree of control can be achieved in the geometry and extent of fractures. If the chemical grout can be made to be the vehicle for the fracturing material, it appears that formation of fractures and impermeation across the fractured planes can be accomplished in one single operation. A synthetic gas storage reservoir formed in the middle of a large body of sandstone where there exists no previous closure or structure is depicted in Fig. 5.8.

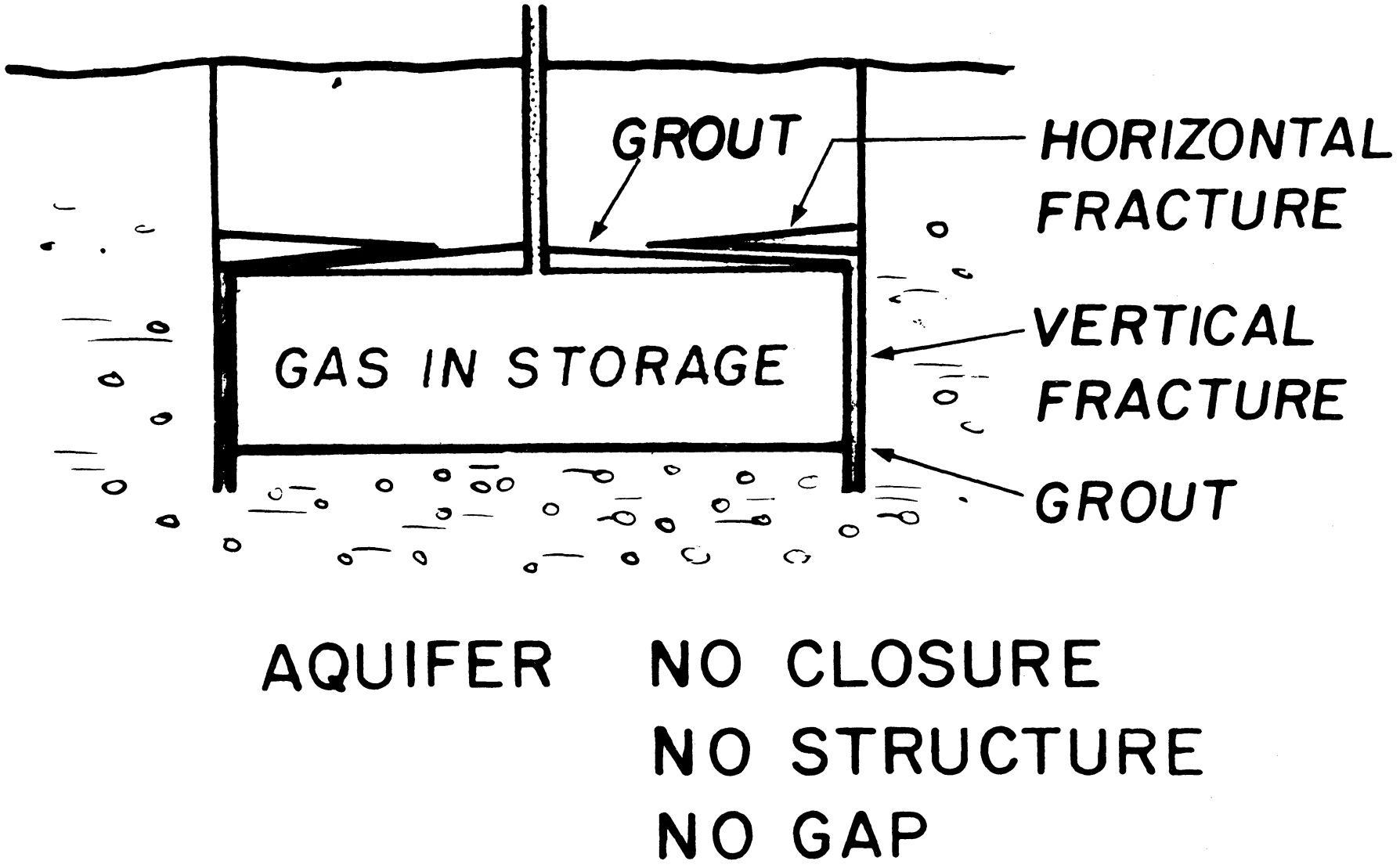

Fig. 5.8. Applications of grouts with fracturing.

REFERENCES

5.1 Carslaw, H. S. and J. C. Jaeger, "Conduction of Heat in Solids," 2nd Ed, Oxford at the Clarendon Press (1959).

5.2 Katz, D. L., M. R. Tek, et al, "Movement of Underground Water in Contact with Natural Gas" (Project No-31) American Gas Association, New York (1963).

CHAPTER 6

UNDERGROUND STORAGE IN NON-POROUS VOID CAVITIES

There are several new means under consideration, some even as far as pilot scale operations, for storage of gas in underground void space. While the engineering possibility and economic feasibility on some of these must depend upon many factors including their size, in areas completely devoid of media for conventional underground storage these non-conventional methods should provide at least substantial peak-shaving capability. These methods will be listed and reviewed in the following:

6.1. Storage in Dissolved Salt Cavities

In areas of high peak demand caverns washed out of salt previously used for storage of liquified petroleum gas have been suggested for the storage of natural gas as well. In 1960 Southeastern Michigan Gas Company began development of an underground storage project in an abandoned solution cavern located near Marysville, Michigan. This cavern has been leached by Morton Salt Company at a depth of 2100 feet. In the operation of such a cavern the pressure of the gas in the cavern is proportional to the quantity of gas in the cavern. During the production of gas from the cavern if each cubic foot of gas removed is replaced by an equal volume of brine, the cavern pressure would remain constant. When large quantities of gas are produced to meet seasonal peak requirements large pumping rates would be required to maintain the cavern pressure constant. If the cavern pressure is allowed to drop to

some safe value, one then can expand the gas out of the cavern without economically and unfeasibly high pumping requirements. In that case the question becomes: how far one can allow the cavern pressure to drop before collapse may occur under the influence of overburden weight? In caverns of irregular shape surrounded by heterogeneous materials, the stress induced in porous media adjacent to the cavern is extremely hard to predict and analyze. Theory of elasticity applied to porous media, anisotropic stress characteristics of formations encountered, co-presence of fluid and solid state stresses further complicate a general solution to this problem. However, there exists some theoretical solution on stress distributions in caverns of idealized geometry and some empirical data from safe pressures observed in field operations. In spherical, conical and cylindrical caverns the stress distribution in the walls becomes a function of the thickness of cap rock supporting the cavern. There exists in the literature some design information on formation and operation of underground salt cavities.[6.1,6.2] In addition to stress and structural stability problems, gas loss from salt caverns due to leakage through permeability of salt particularly when dry or through incipient fractures must be considered carefully in addition to loss of gas which dissolves in the brine pumped out. A schematic sketch of such a cavern is shown in Fig. 6.1.

6.2. Storage in Natural, Mined or Nuclear Explosion Induced Cavities

There are 11,791 known caves in the United States.[6.3] Some of these are known to be over 400 feet deep, to cover acres of subsurface area and interconnected through miles and miles of tortuous passage ways. Most of the caverns are formed in limestone beds through dissolving action of underground

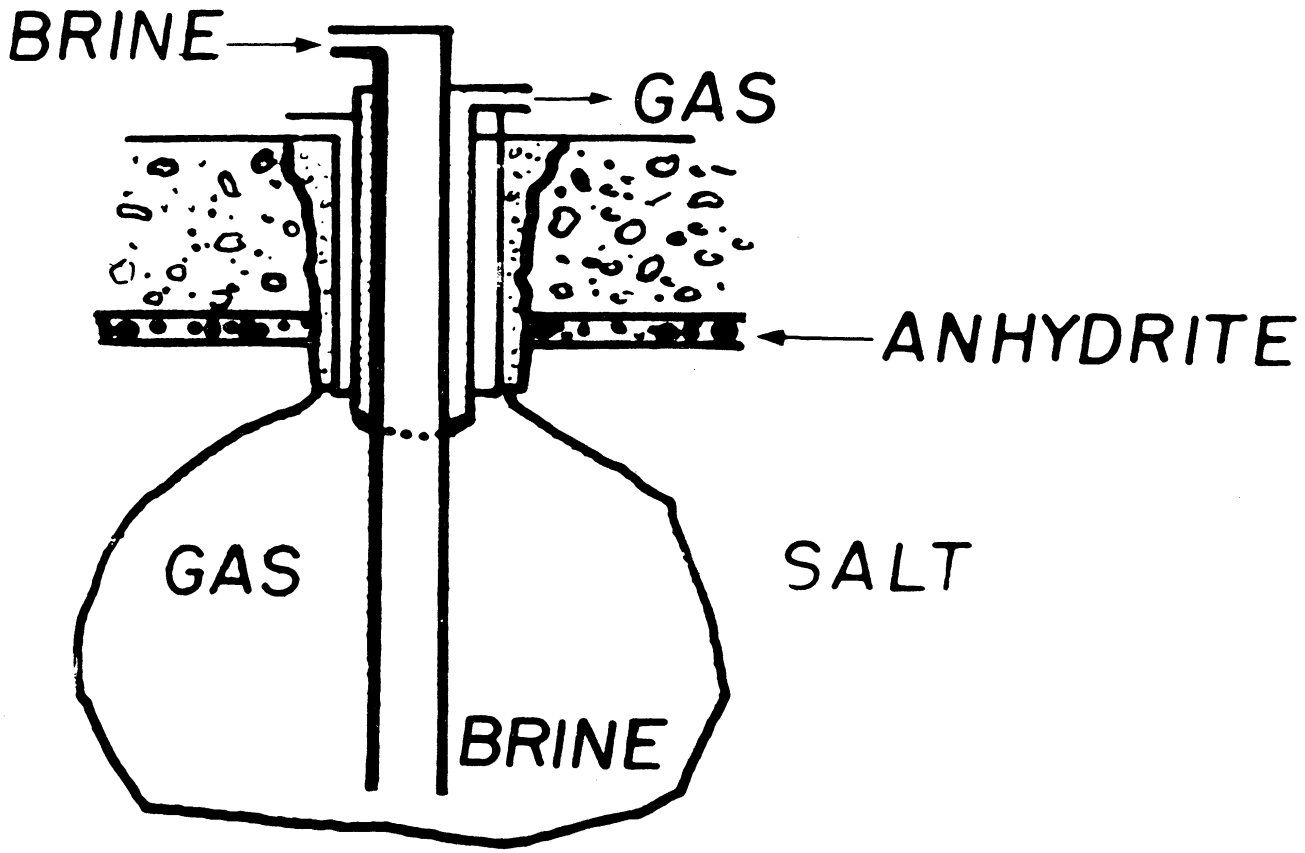

Fig. 6.1. Salt cavern storage.

water combined with stream erosion and subsequent drying as the level of underground water table drops. The prospect of storing natural gas in caverns located near areas of great need for storage depends upon many factors. The maximum pressure that can be safely carried in the caverns, the condition of cavern walls with respect to permeability, incipient fractures and groutability, the nature and condition of overburden above the cavern must all be considered before their economic feasibility can be assessed. The problems in mined caverns are quite similar to those of natural caverns. There has been some use in the United States of abandoned coal mines for the storage of natural gas.

The proximity of mined or natural caverns near the surface creates a serious limitation for their storage capacity due to the maximum pressure that can be used as related to the formation parting pressure at the ceiling of the cavern. This limitation is not present in the prospect of using a cavern induced by nuclear explosion at some satisfactory depth for the storage of natural gas. It is interesting to note that in a shallow cavity the primary limitation for storage is the maximum pressure while in a deep cavity the controlling limit is probably the minimum pressure. Throughout the recent years considerable engineering and research effort has been deployed toward the technology and analysis of subsurface nuclear explosions.[6.4,6.5] The data collected in various experiments have been analyzed with a view toward possible use of caverns created in the storage of natural gas.

Five of the specific subsurface neuclear experiments have been of particular interest. These are "Event Rainier," the first major nuclear explo-

sion completely contained underground, "Event Logan," specially conducted to get seismic data and "events" "Blanca," "Gnome" and "Hardhat." The major program to which the above five experiments belonged was called "Project Plowshare." A study of the data reported on the five events indicate that the "Event Gnome" was the first contained nuclear explosion which created a deep cavity which did not collapse. In that particular experiment the fact that an aquifer situated 650 feet above the device which exploded and a tunnel shaft located 1300 feet from the explosion were not damaged is of particular interest.

When a nuclear explosion occurs underground it may be a cratering or contained event depending upon many factors. A cratering explosion is characterized by the eruption of blast into the atmosphere. A contained event shows very little surface effects. Empirical data collected from Project Plowshare indicates that the depth of a contained explosion is a direct function of the yield of explosion:

$$H = 350\ W^{1/3}$$

where: H = minimum depth of exploding device for containment, feet

W = yield of the device, kilotons.

In a contained nuclear explosion the shape and size of the cavity obtained depend on properties of subsurface area near the shot, the depth of exploding device, yield of explosion. The yield of nuclear energy causing an adiabatic shock wave attended by temperature and pressures in the order of million degrees F and million atmospheres, propagation of the shock wave to the surface and reflection down to the cavity, first vaporization then condensation and

flow of molten phase, all result in a stable, approximately spherical cavity if the internal pressure can hold-up both the overburden weight and the shock wave returing from the surface. Otherwise the phenomenon called "chimney formation" will occur where the roof collapses leaving the cavity full of rubble. The chimney may or may not extend to the surface.

The "Gnome Event" resulted in a stable cavity of nearly spherical shape with an average radius of 87 ft in average radius at a depth of 1200 ft. If gas pressures up to 1 psi/ft could be maintained in such a cavity the approximate amount of natural gas in storage would be about 290 MMCF. For a cavity twice the size at twice the depth, the storage capacity would be about 5 billion standard cubic feet. The nature of the interior surface of the cavity, its impermeability, threshold pressure, susceptibility to fractures during drilling or due to overpressure, the decay of radiation and many other problems must be carefully and exhaustively considered before the economics of gas storage in nuclear cavities can begin to crystallize.

6.3. Underwater Storage of Natural Gas

One of the most recent and promising ideas advanced at The University of Michigan research project on new concepts is the storage of natural gas at the bottom of lakes or oceans. The sea offers interesting advantages over methods of conventional underground storage because of the following reasons:

1. More storage space per bulk storage volume (100 percent porosity)
2. Availability of pressure for storage.
3. Minimum safety, leakage, collection, contamination problems.

4. Low and constant temperature of ocean bottom permitting more gas to be stored for same depth and pressure.

5. Presence of salt water which would prevent hydrate formation.

6. Possibility to practice overpressuring in special containers to a much larger extent than in underground storage.

Figure 6.2 represents our current conception for a peak shaving storage installation located at the bottom of the ocean at some suitable depth. It merely and simply consists of an inverted container open at the bottom and supplied from the top by a pipeline. As the pressure in the pipeline is increased the natural gas flows in the container pushing the sea water out. During periods of peak demand as the gas is pulled through the distribution network, the water moves in and displaces the gas out. One of the critical requirements of such a storage facility is to provide suitable and sufficient anchor design to hold the container and the pipeline at the bottom.

Figure 6.3 shows the reservoir volume necessary to store one billion standard cubic feet of natural gas under water as a function of depth. It can be seen that 0.6 gravity gas at 3000 feet, one would need a container having a volume of 7.8×10^6 cubic feet. A vessel of spherical shape open at the bottom of this volume would have a radius of about 125 feet. The total anchoring force to hold such a vessel at the bottom would be equal to about 4.8×10^8 pounds-force as can be seen from Fig. 6.4. While these anchoring requirements seem to be enormous at first with the rapidly advancing underwater construction technology, it is believed that mechanical and design problems associated with underwater storage are definitely within the reach of mechanically possible and economically feasible solutions.

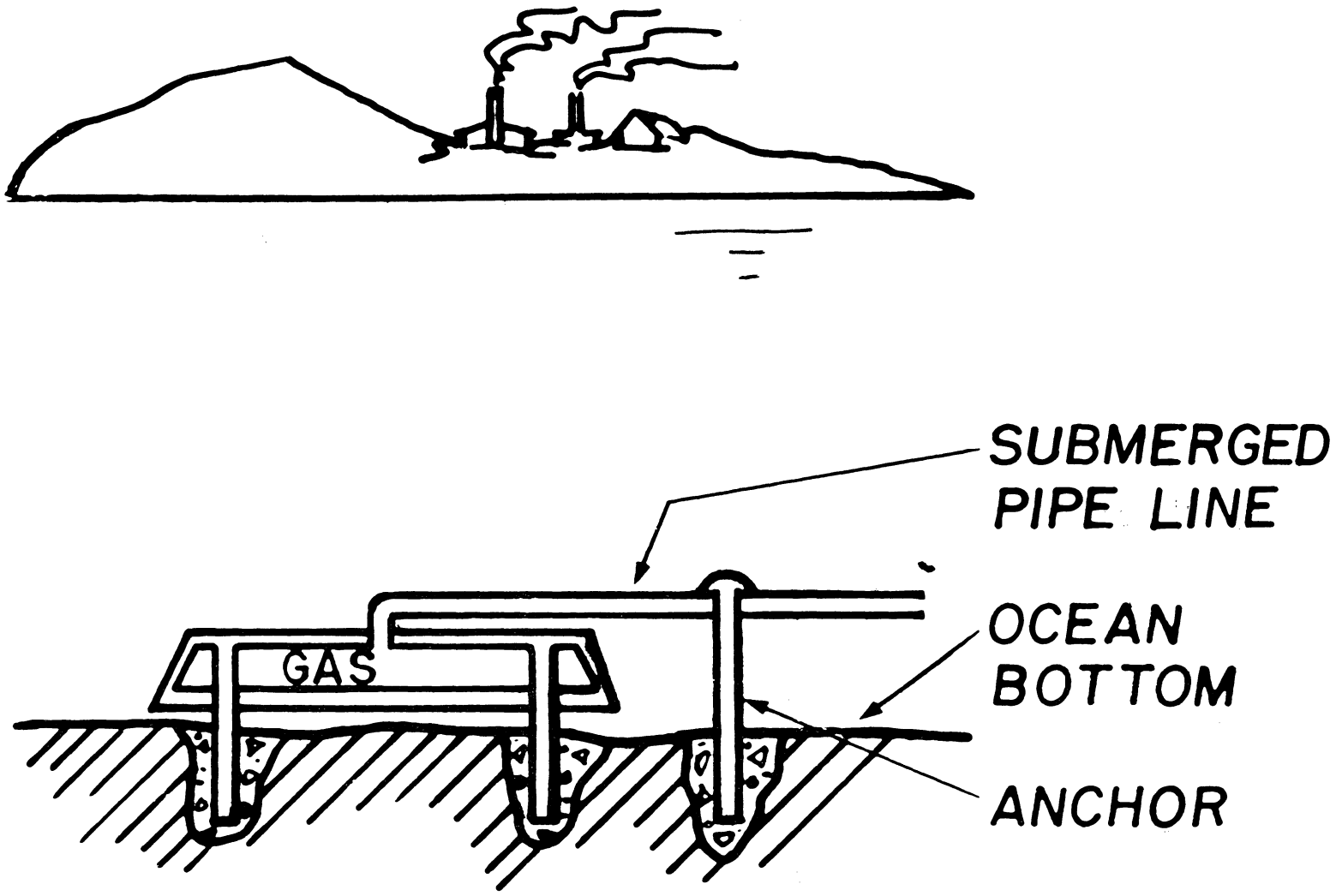

Fig. 6.2. Peak shaving storage at ocean bottom.

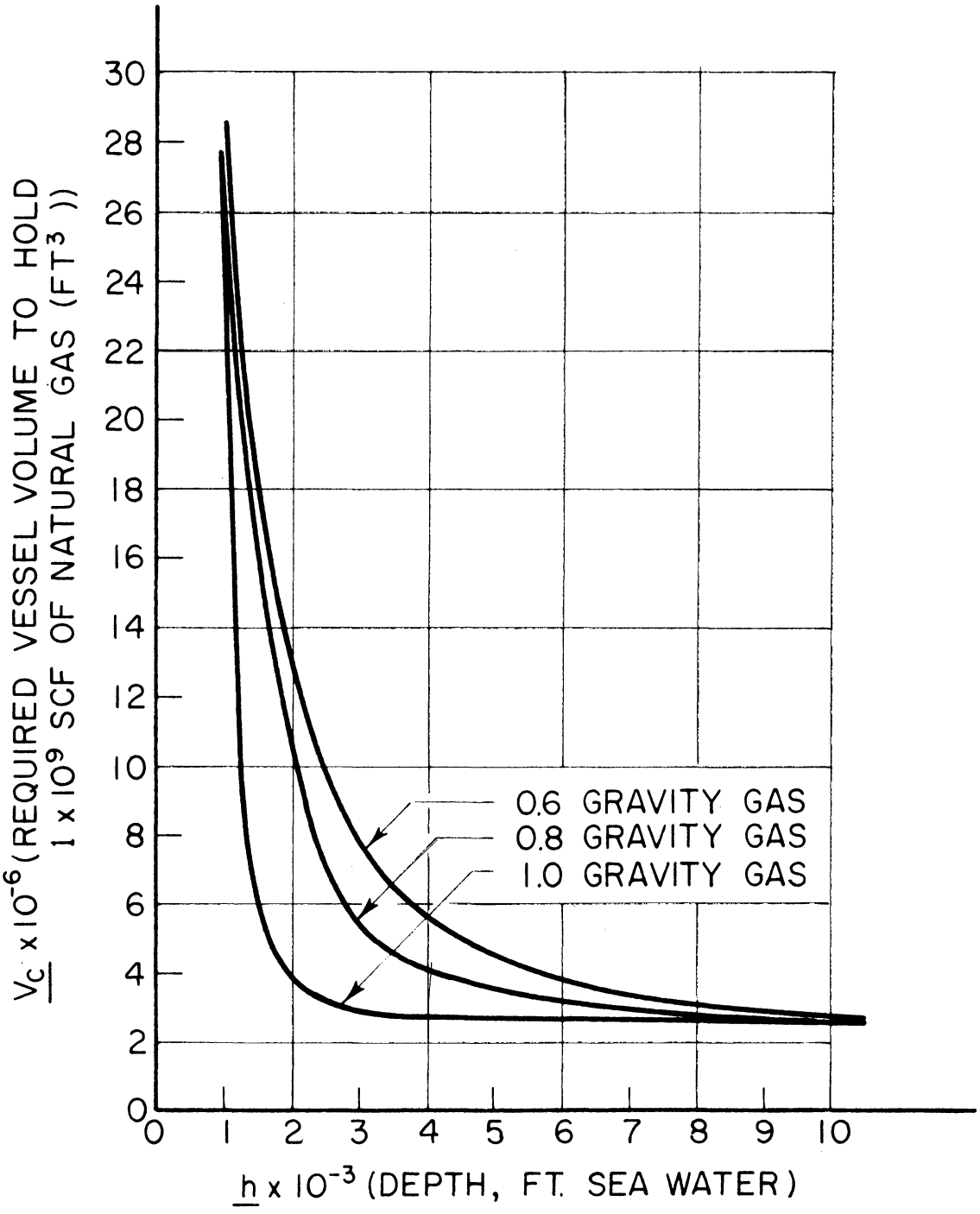

Fig. 6.3. Reservoir volume vs. depth necessary to store 10^9 SCF of natural gas in sea water.

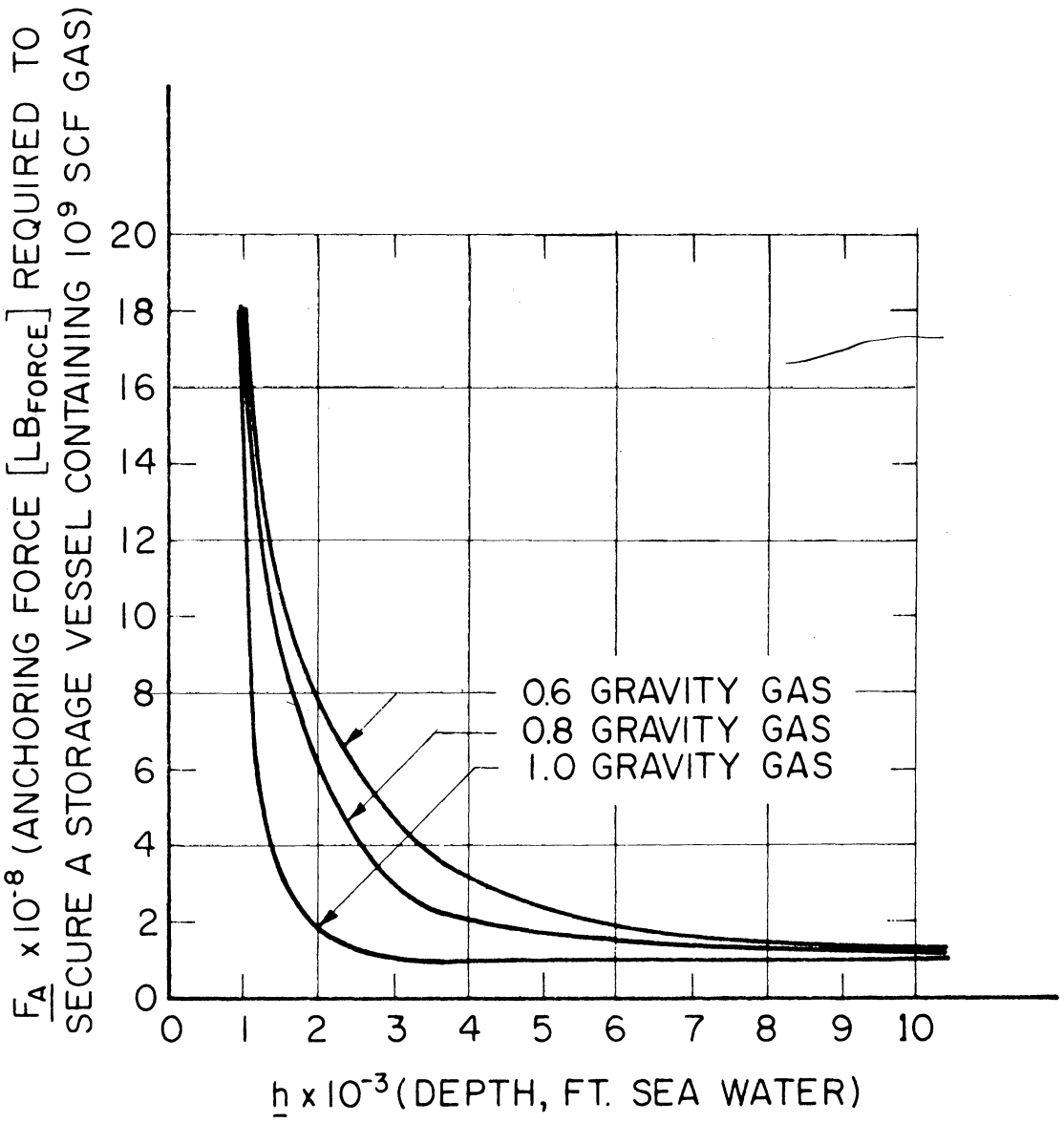

Fig. 6.4. Anchoring force requirements for 10^9 SCF vessel in sea water.

REFERENCES

6.1 Serata Shosei and Gloyna, E., Design Principles for Underground Salt Cavities, ASCE Trans., Paper 3146 (1961)

6.2 Johns, D. F., Formation Strength in Salt Cavern Storage, Petroleum Engineer, August 1957.

6.3 Charles E. Mohr, "Exploring America Underground," National Geographic Magazine, 125, 6, 803 June (1964).

6.4 Ralph Sanden, Project Plowshare, Public Affairs Press, Washington D. C. (1962).

6.5 AEC Reports, UCRL - 5675, 5676, 6588, 6240.